



THE UNIVERSITY *of* EDINBURGH

Edinburgh Research Explorer

Genomic and drug target evaluation of 90 cardiovascular proteins in 30,931 individuals

Citation for published version:

Folkersen, L, Gustafsson, S, Wang, Q, Hansen, DH, Hedman, AK, Schork, AW, Page, K, Zernakova, DV, Wu, Y, Peters, J, Eriksson, N, Bergen, SE, Boutin, T, Bretherick, AD, Enroth, S, Kalnapenkis, A, Gádin, JR, Suur, B, Chen, Y, Matic, L, Gale, JD, Lee, J, Zhang, W, Quazi, A, Ala-Korpela, M, Choi, SH, Claringbould, A, Danesh, J, Davey Smith, G, o de Masi, F, Elmstahl, S, Engström, G, Fauman, E, Fernandez, C, Franke, L, Franks, P, Giedraitis, V, Haley, C, Hayward, C, Wilson, JF, Wallentin, L, Butterworth, AS, Holmes, MV, Ingelsson, E & Mälarstig, A 2020, 'Genomic and drug target evaluation of 90 cardiovascular proteins in 30,931 individuals', *Nature Metabolism*. <https://doi.org/10.1038/s42255-020-00287-2>

Digital Object Identifier (DOI):

<https://doi.org/10.1038/s42255-020-00287-2>

Link:

[Link to publication record in Edinburgh Research Explorer](#)

Document Version:

Peer reviewed version

Published In:

Nature Metabolism

General rights

Copyright for the publications made accessible via the Edinburgh Research Explorer is retained by the author(s) and / or other copyright owners and it is a condition of accessing these publications that users recognise and abide by the legal requirements associated with these rights.

Take down policy

The University of Edinburgh has made every reasonable effort to ensure that Edinburgh Research Explorer content complies with UK legislation. If you believe that the public display of this file breaches copyright please contact openaccess@ed.ac.uk providing details, and we will remove access to the work immediately and investigate your claim.



Genomic evaluation of circulating proteins for drug target characterisation and precision medicine

Lasse Folkersen^{1,2*}, Stefan Gustafsson^{3*}, Qin Wang^{4,5*}, Daniel Hvidberg Hansen⁶, Åsa K Hedman^{2,7}, Andrew Schork^{1,8}, Karen Page⁹, Daria V Zhernakova¹⁰, Yang Wu¹¹, James Peters¹², Niclas Eriksson¹³, Sarah E Bergen¹⁴, Thibaud Boutin¹⁵, Andrew D Bretherick¹⁵, Stefan Enroth¹⁶, Anette Kalnapenkis¹⁷, Jesper R Gådin², Bianca Suur¹⁸, Yan Chen², Ljubica Matic¹⁸, Jeremy D Gale¹⁹, Julie Lee⁹, Weidong Zhang²⁰, Amira Quazi⁹, Mika Ala-Korpela^{4,5,21}, Seung Hoan Choi²², Anniqe Claringbould¹⁰, John Danesh¹², George Davey-Smith²³, Federico de Masi⁶, Sölve Elmståhl²⁴, Gunnar Engström²⁴, Eric Fauman²⁵, Celine Fernandez²⁴, Lude Franke¹⁰, Paul Franks²⁶, Vilmantas Giedraitis²⁷, Chris Haley¹⁵, Anders Hamsten², Andres Ingason¹, Åsa Johansson¹⁶, Peter K Joshi²⁸, Lars Lind²⁹, Cecilia M. Lindgren^{30,31,22}, Steven Lubitz^{32,22}, Tom Palmer³³, Erin Macdonald-Dunlop²⁸, Martin Magnusson^{34,35}, Olle Melander²⁴, Karl Michaelsson³⁶, Andrew P. Morris^{37,38,31}, Reedik Mägi¹⁷, Michael Nagle²⁵, Peter M Nilsson²⁴, Jan Nilsson²⁴, Marju Orho-Melander³⁹, Ozren Polasek⁴⁰, Bram Prins¹², Erik Pålsson⁴¹, Ting Qi¹¹, Marketa Sjögren²⁴, Johan Sundström⁴², Praveen Surendran¹², Urmo Vösa¹⁷, Thomas Werge¹, Rasmus Wernersson⁶, Harm-Jan Westra¹⁰, Jian Yang^{11,43}, Alexandra Zhernakova¹⁰, Johan Ärnlöv⁴⁴, Jinyuan Fu¹⁰, Gustav Smith⁴⁵, Tonu Esko^{17,22}, Caroline Hayward¹⁵, Ulf Gyllenstein¹⁶, Mikael Landén⁴¹, Agnetta Siegbahn⁴⁶, Jim F Wilson^{28,15}, Lars Wallentin⁴⁷, Adam S Butterworth¹², Michael V Holmes^{48*}, Erik Ingelsson^{49*}, Anders Mälarstig^{2,50*}

* these authors contributed equally

1 Institute of Biological Psychiatry, Mental Health Center Sct. Hans, Mental Health Services Capital Region, Roskilde, Denmark

2 Department of Medicine, Solna, Karolinska Institute, Sweden

3 Department of Medical Sciences, Molecular Epidemiology and Science for Life Laboratory, Uppsala University, Uppsala, Sweden

4 Systems Epidemiology, Baker Heart and Diabetes Institute, Melbourne, VIC, Australia

5 Computational Medicine, Faculty of Medicine, University of Oulu and Biocenter Oulu, Oulu, Finland

6 Intomics, Lottenborgvej 26, 2800 Lyngby (Copenhagen), Denmark

7 Pfizer Worldwide Research & Development, Cambridge, MA, USA

8 Neurogenomics Division, The Translational Genomics Research Institute (TGEN), Phoenix, AZ, USA

9 Early Clinical Development, Pfizer Worldwide Research & Development, Cambridge, MA, USA

10 Department of Genetics, University of Groningen, University Medical Center Groningen, Groningen, the Netherlands

11 Institute for Molecular Bioscience, The University of Queensland, Brisbane, Queensland, Australia

12 BHF Cardiovascular Epidemiology Unit, Department of Public Health and Primary Care, University of Cambridge, United Kingdom

13 Department of Medical Sciences, Uppsala Clinical Research Center, Uppsala University, Uppsala, Sweden

14 Department of Medical Epidemiology and Biostatistics, Karolinska Institutet, Stockholm, Sweden

15 MRC Human Genetics Unit, Institute of Genetics and Molecular Medicine, University of Edinburgh, Western General Hospital, Crewe Road, Edinburgh, EH4 2XU, Scotland

16 Department of Immunology, Genetics, and Pathology, Biomedical Center, Science for Life Laboratory (SciLifeLab) Uppsala, Box 815, Uppsala University, SE-75108 Uppsala, Sweden

17 Estonian Genome Center, Institute of Genomics, University of Tartu 51010, Estonia

18 Department of Molecular Medicine and Surgery, Solna, Karolinska Institute, Sweden

19 Inflammation and Immunology Research Unit, Pfizer Worldwide Research & Development, Cambridge, MA, USA

20 Pfizer Global Product Development, Cambridge, MA, USA

21 NMR Metabolomics Laboratory, School of Pharmacy, University of Eastern Finland, Kuopio, Finland

22 Program in Medical and Population Genetics, Broad Institute, Cambridge, MA, USA

23 MRC Integrative Epidemiology Unit, University of Bristol, UK

24 Department of Clinical Sciences, Lund University, Skåne University Hospital, Malmö, Sweden

25 Internal Medicine Research Unit, Pfizer Worldwide Research & Development, Cambridge, MA, USA

26 Lund University Diabetes Center, Department of Clinical Sciences, Malmö, Sweden

27 Department of Public Health and Caring Sciences/Geriatrics, Uppsala University, Uppsala, Sweden.

28 Centre for Global Health Research, Usher Institute for Population Health Sciences and Informatics, University of Edinburgh, Teviot Place, Edinburgh, EH8 9AG, Scotland

29 Department of Medical Sciences, Uppsala University, Uppsala, Sweden.

30 Big Data Institute at the Li Ka Shing Centre for Health Information and Discovery, University of Oxford, Oxford, United Kingdom.

31 Wellcome Centre for Human Genetics, Nuffield Department of Medicine, University of Oxford, Oxford, United Kingdom.

32 Cardiovascular Research Center, Massachusetts General Hospital, United States.

33 Department of Mathematics and Statistics, University of Lancaster, Lancaster, UK

34 Department of Cardiology, Skåne University Hospital Malmö, Malmö, Sweden

35 Wallenberg Center for Molecular Medicine, Lund University, Lund, Sweden

36 Department of Surgical Sciences, Uppsala University, Uppsala, Sweden

37 Division of Musculoskeletal and Dermatological Sciences, University of Manchester, Manchester, UK

38 Department of Biostatistics, University of Liverpool, Liverpool, UK

39 Department of Clinical Sciences, Clinical Research Center, Lund University, Malmö, Sweden

64 40 Faculty of Medicine, University of Split, Split, Croatia
65 41 Department of Psychiatry and Neurochemistry, Institute of Neuroscience and Physiology, the Sahlgrenska Academy at the University of Gothenburg, Gothenburg, Sweden
66
67 42 Department of Medical Sciences, Clinical Epidemiology, Uppsala University, Uppsala, Sweden; and The George Institute for Global Health, University of New
68 South Wales, Sydney, Australia
69 43 Institute for Advanced Research, Wenzhou Medical University, Wenzhou, Zhejiang 325027, China
70 44 Department of Neurobiology, Care Sciences and Society (NVS), Division of Family Medicine and Primary Care, Karolinska Institutet, Sweden
71 45 Department of Cardiology, Clinical Sciences, Lund University, Skåne University Hospital, Lund, Sweden.
72 46 Department of Medical Sciences, Clinical Chemistry, Uppsala University, Uppsala, Sweden
73 47 Department of Medical Sciences, Cardiology and Uppsala Clinical Research Center, Uppsala University, Uppsala, Sweden
74 48 Clinical Trial Service Unit and Epidemiological Studies Unit (CTSU), Nuffield Department of Population Health, University of Oxford, Oxford, United Kingdom.
75
76 49 Department of Medicine, Division of Cardiovascular Medicine, Falk Cardiovascular Research Center, Stanford University School of Medicine, 300 Pasteur Drive, CV 273, Stanford, CA, 94305, USA.
77
78 50 Emerging Science & Innovation, Pfizer Worldwide Research & Development, Cambridge, MA, USA
79

80

81 **Abstract**

82

83 Circulating proteins are vital in human health and disease and are frequently used as biomarkers for
84 clinical decision-making or as targets for pharmacological intervention. By mapping and replicating
85 protein quantitative trait loci (pQTL) for 90 cardiovascular proteins in over 30,000 individuals, we
86 identified 451 pQTLs for 85 proteins. The pQTLs were used in combination with other sources of
87 information to evaluate known drug targets, and suggest new target candidates or repositioning
88 opportunities, underpinned by a) causality assessment using Mendelian randomization, b) pathway
89 mapping using *trans*-pQTL gene assignments, and c) protein-centric polygenic risk scores enabling
90 matching of plausible target mechanisms to sub-groups of individuals enabling precision medicine.

91

92

93

94

95

96

97

98

99

100

101 Main

102 Proteins circulating in blood are derived from multiple organs and cell types, and consist of both
103 actively secreted and passively leaked proteins. Plasma proteins are frequently used as biomarkers to
104 diagnose and predict disease and have been of key importance for clinical practice and drug
105 development for many decades.

106 Circulating proteins are attractive as potential drug targets as they can often be directly perturbed
107 using conventional small molecules or biologics such as monoclonal antibodies¹. However, a
108 prerequisite for successful drug development is efficacy, which is predicated on the drug target
109 playing a causal role in disease. One approach to clarifying causation is through Mendelian
110 randomization (MR), which has successfully predicted the outcome of randomized controlled trials
111 (RCT) for pharmacological targets such as PCSK9, LpPLA2 and NPC1L1, and is increasingly becoming a
112 standard tool for triaging new drug targets².

113 Recent technological developments of targeted proteomic methods have enabled hundreds to
114 thousands of circulating proteins to be measured simultaneously in large studies³⁻⁶. This has paved
115 the way for studies of genetic regulation of circulating proteins using genome-wide association
116 studies (GWAS) for detection of protein quantitative trait loci (pQTL), some of which are referenced
117 here^{3,4,7-9}.

118 Here, we present a genome-wide meta-analysis of 90 cardiovascular-related proteins, many of which
119 are established prognostic biomarkers or drug targets, measured using the Olink Proximity Extension
120 Assay CVD-I panel¹⁰ in 30,931 subjects across 14 studies. The identified pQTLs were combined with
121 other sources of information to suggest new target candidates underpinned by insights into *cis*- and
122 *trans*- regulation of protein levels and to evaluate past and present efforts to therapeutically modify
123 the proteins analysed in the present investigation. We also show that protein-centric polygenic risk
124 scores (PRS) can predict a substantial fraction of inter-individual variability in circulating protein
125 levels, explaining a proportion of disease susceptibility attributable to specific biological pathways.

126 These are the first results to emerge from the SCALLOP consortium, a collaborative framework for
127 pQTL mapping and biomarker analysis of proteins on the Olink platform (www.scallop-
128 consortium.com).

129 Results

130 Genome-wide meta-analysis of 90 proteins reveals 467 independent genetic loci 131 associated with plasma levels of 85 proteins.

132 Ninety proteins in up to 21,758 participants from 13 cohorts passed quality control (QC) criteria and
133 were available for GWAS meta-analysis [Supplementary Table 1]. We found a total of 401 pQTLs that
134 were significant at a discovery P -value threshold conventional for GWAS ($P < 5 \times 10^{-8}$). [Supplementary
135 Table 2]. Conditioning each of these primary pQTLs using the GCTA-COJO software, we identified an
136 additional 144 proximal pQTLs that independently surpassed conventional genome-wide significance
137 ($P < 5 \times 10^{-8}$), termed as secondary pQTLs. We attempted to replicate the primary and secondary pQTLs
138 in two independent studies (9,173 participants) whereupon the discovery and replication datasets
139 were meta-analysed, leading to 315 primary pQTLs and 136 secondary pQTLs surpassing a Bonferroni
140 corrected P -value ($P < 5.6 \times 10^{-10}$). The discovery P -values were used for pQTLs absent in the replication
141 dataset ($n_{\text{snp}}=25$) [Supplementary Table 2].

142 Some proteins such as SCF, RAGE, PAPPA, CTSL1 and MPO showed association with more than nine
143 primary pQTLs, but most proteins (22 of 85) were associated with 2 primary pQTLs. We also observed
144 that some proteins were associated with multiple conditionally significant (secondary) pQTLs such as
145 CCL-4 with 4 secondary signals, implicating complex genetic regulation of circulating CCL-4 at the
146 *CCL4* locus.

147 Analysis of *trans*-pQTLs suggests common mechanisms by which genetic variants 148 affect plasma protein levels.

149 A “best guess” causal gene for each of the CVD-I *trans*-pQTLs was assigned by a hierarchical approach
150 based on analysis of protein-protein interactions (PPI), literature mining, genomic distance to gene
151 and manual review of literature around the gene as well as the genomic context of the association

152 signal. In total, 326 primary trans-pQTLs were assigned to unique genes and 30 trans-pQTLs were
153 assigned more than one gene, with *ABO*, *ST3GAL4*, *JMJD1C*, *SH2B3*, *ZFPM2* showing association with
154 the levels of five or more CVD-I proteins [Supplementary Figure 2B] [Supplementary Table 2].
155 Extending this analysis to pQTLs from literature expanded the list of genes with five or more protein
156 associations to include also *KLKB1*, *GCKR*, *FUT2*, *TRIB1*, *SORT1* and *F12* [Supplementary Table 4].
157 Gene ontology (GO) analysis of genes assigned to all significant trans-pQTLs showed functional
158 enrichment for chemokine binding, glycosaminoglycan binding, receptor binding and G-protein
159 coupled chemoattractant activity [Figure 2C]. A broader classification of genes assigned to both cis-
160 and trans-pQTLs [Figure 2A, 2B] [Supplementary Table 2] using a wider set of tools (Online Methods)
161 suggested that transcriptional regulation, post-translational modifications, such as glycation and
162 sialylation, cell-signalling events, protease activity and receptor binding are potential common
163 mechanisms by which trans-pQTLs influence circulating protein levels. The default gene calls and
164 paths for the CVD-I *trans*-pQTLs based on PPI and literature mining can be visualised using the
165 [SCALLOP CVD-I network tool](#) [Supplementary Figure 2B] whereas details on the classification of genes
166 are available in the Online Methods.

167 Evidence of mRNA expression mediating associations with a third of cis pQTLs

168 We investigated the overlap of the CVD-I *cis*- and *trans*-pQTLs with expression quantitative trait loci
169 (eQTL) by a combination of approaches and eQTL studies, including direct genetic lookups and co-
170 localisation using PrediXcan¹¹ and SMR / HEIDI¹². For direct lookups, three studies were used:
171 LifeLines-DEEP (whole blood), eQTLGen meta-analysis (whole blood and PBMCs) and GTEx (48 tissue
172 types). Of 545 pQTLs from supplementary table 2, eQTL data were available for 434 SNP-transcript
173 pairs, including 168 *cis*-pQTLs and 266 *trans*-pQTLs. Of these, 72 (43%) of *cis*-pQTLs had at least one
174 corresponding eQTL (FDR<0.05) in any of the eQTL datasets investigated, implicating 42 of the 75
175 proteins with a *cis*-pQTL. At a more stringent eQTL p-value of $P < 5 \times 10^{-8}$, the percentage with a
176 corresponding eQTL was 26 %, similar to some previous reports¹³⁻¹⁵ [Supplementary Table 5].

177 Co-localisation analysis of CVD-I cis-pQTLs and mRNA levels was performed in selected tissues from
178 the GTEx project by first imputing mRNA expression of the CVD-I protein-encoding transcripts using
179 the PrediXcan¹¹ algorithm in one of the SCALLOP CVD-I cohorts (IMPROVE), and then testing imputed
180 mRNA levels for association with CVD-I plasma protein levels using linear regression. Twenty-six of
181 the 90 CVD-I proteins were associated with their corresponding mRNA transcript (FDR<0.05) in at
182 least one of the 20 GTEx tissues investigated [Supplementary Figure 3]. All 26 proteins were among
183 the 42 proteins found to also be an eQTL by direct lookups. Proteins CCL4, CD40, CHI3L1, CSTB and
184 IL-6RA all associated with their corresponding transcript across five or more tissues whereas proteins
185 ST2 and RAGE showed significant association exclusively in lung, and CTSD exclusively in skeletal
186 muscle.

187 To further investigate if the CVD-I protein pQTLs overlap with eQTLs, we used the SMR/HEIDI
188 methods¹², using data from the Consortium for the Architecture of Gene Expression (CAGE) study.
189 SMR/HEIDI tests the hypothesis that there is a single variant affecting protein and gene expression
190 (pleiotropy or causality), with the alternative hypothesis being that protein and gene expression are
191 affected by two distinct variants. In total, 125 associations between 96 genes and 54 proteins were
192 identified at an experiment-wise SMR test significance level ($P_{SMR} < 0.05/8558$) and a stringent HEIDI
193 test threshold ($P_{HEIDI} > 0.01$) [Supplementary Table 6], of which 23.2 % were in *cis*-pQTL regions, such
194 as IL-8 and U-PAR. The 96 genes were located in 74 loci, suggesting that pleiotropic associations
195 between protein and mRNA expression were present for 18.4 % of significant and suggestive primary
196 loci using SMR / HEIDI.

197 **A minor proportion of *cis*-acting pQTLs are in high linkage-disequilibrium with** 198 **non-synonymous coding variants.**

199 “Pseudo-pQTLs” caused by epitope effects, i.e. differential assay recognition depending on presence
200 of protein-altering variants, is a theoretical possibility for *cis*-pQTLs and likely dependent on the
201 method of protein quantification^{4,16}. To evaluate the potential for pseudo-pQTLs among the CVD-I
202 pQTLs, we investigated presence of protein-altering variants for sentinel variants or variants in high

203 linkage disequilibrium with a sentinel variant. Of the 90 proteins, 85 had at least one pQTL, including
204 12 with only *cis*-pQTLs, 10 with only *trans*-pQTLs and 63 with both *cis*- and *trans*-pQTLs. Of the 170
205 primary or secondary *cis*-pQTLs for 75 proteins, 20 *cis*-pQTLs for 18 proteins had a sentinel variant in
206 high linkage disequilibrium (LD; $R^2 > 0.9$) with a protein-altering variant, which suggests potential to
207 affect assay performance [Supplementary Table 1].

208 Orthogonal evidence supports causal gene to protein relationships for a subset of 209 the CVD-I *trans*-pQTLs

210 Of the 326 *trans*-pQTLs identified, eight were assigned to gene products targeted by compounds or
211 antibodies that have been in clinical development [Supplementary Table 7]. Assuming that *trans*-
212 pQTLs represent causal relationships between gene variants and proteins, we hypothesized that the
213 downstream CVD-I proteins associated with CVD-I *trans*-pQTL genes would be modulated on
214 therapeutic modification of the gene product. Support for this hypothesis was obtained by previous
215 work showing that circulating FABP4 is upregulated upon treatment with glitazones (PPARG
216 inhibitors)¹⁷; that circulating IL-6 is increased after treatment with tocilizumab¹⁸ (IL6R inhibitor) and
217 that circulating TNF-R2 is decreased upon infliximab (TNFA inhibitor) treatment in patients with
218 Crohn's disease¹⁹, which supports CVD-I *trans*-pQTLs for these proteins. Along these lines, we present
219 novel evidence from a clinical trial supporting our observations that a CCR5 variant is a *trans*-pQTL
220 for plasma CCL-4 and a variant in CCR2 is a *trans*-pQTL for plasma MCP-1 [Supplementary table 2].
221 CCR5 and CCR2 are targeted in combination by the small-molecule dual-inhibitor PF-04634817²⁰. To
222 test whether dual inhibition of CCR5 and CCR2 resulted in a change of circulating CCL-4 and MCP-1
223 respectively, we measured these proteins in 350 type 2 diabetes patients in a randomized, double-
224 blind, placebo-controlled phase-II trial evaluating the efficacy of PF-04634817 in diabetic
225 nephropathy (NCT01712061). In addition, we also measured known or suspected ligands of CCR5 and
226 CCR2, including CCL-3, CCL-5 (RANTES) and CCL-8, and 5 additional proteins that were present on the
227 Olink CVD-I panel, and for which assays were readily available. Compared to placebo, we observed a
228 9.25-fold increase in circulating MCP-1 levels ($p < 0.0001$) and a 2.11-fold increase in circulating CCL4

229 levels ($p < 0.0001$) at week 12 [Figure 3]. An alternative ligand for CCR-2; CCL-8 did not change
230 following exposure to PF-04634817, and neither did other CCR-5 ligands, such as CCL-5 (RANTES) and
231 CCL-3. Moreover, EN-RAGE, FGF-23, KIM-1, myoglobin and TNFR-2 were unchanged following PF-
232 04634817 exposure [Supplementary Figure 4]. We conclude that CVD-I *trans*-pQTLs at *CCR5* and
233 *CCR2* were concordant with the effects of PF-04634817 in human.

234 Two of the genes implicated by CVD-I *trans*-pQTLs, *ABCA1* and *TRIB1* for circulating SCF levels, were
235 also investigated in the mouse. Mice with liver-specific or whole-body knockdown of *ABCA1*²¹ and
236 *TRIB1*²² respectively showed decreased plasma levels of SCF compared to matched wild-type controls
237 [Figure 4], concordant with the human CVD-I *trans*-pQTLs.

238 Mendelian randomization analysis revealed 25 CVD-I proteins causal for at least 239 one human complex disease or phenotype with strong evidence.

240 To identify potential causal disease pathways indexed by proteins, we conducted an MR analysis of
241 85 proteins across 38 outcomes. 25 proteins showed strong evidence of causality for at least one
242 disease or phenotype and an additional 24 proteins showed intermediate evidence of causality.
243 [Figure 5A; Supplementary Figure 5]. Using open-source information (clinicaltrials.gov)
244 (www.ebi.ac.uk/chembl/) (www.drugbank.ca/) (www.opentargets.org) and Clarivate Integrity
245 (integrity.clarivate.com), we identified records on past or present clinical drug development
246 programs for 14 of the 25 proteins, all of which have been in phase 2 trials or later [Supplementary
247 Table 7]. Of the 14 proteins, seven proteins were targeted for an indication different from the
248 phenotype implicated by our MR analysis. Eleven of the 25 proteins have never been targeted in
249 clinical trials, but may provide new promising target candidates for indications closely related to the
250 traits in the MR analysis.

251 Several published MR findings were confirmed, including that *IL6RA* variants associated with higher
252 circulating levels of interleukin-6 (IL-6) and soluble IL6-RA were associated with lower risk of coronary
253 heart disease (CHD), rheumatoid arthritis (RA) and atrial fibrillation but higher risks of atopy, such as

254 asthma and eczema²³. We also replicated previous findings suggesting a causal contribution of IL-1ra
255 to rheumatoid arthritis (RA) but an inverse causal relationship with cholesterol levels²⁴, and a
256 protective role of genetically higher MMP-12 against stroke^{4,25}.

257 Some novel MR observations included higher levels of CD40 protein and increased risk of RA, higher
258 MMP-12 and increased risk of eczema, and higher TRAIL-R2 proteins levels and prostate cancer.
259 Further, Dkk-1 has been targeted by a humanised monoclonal antibody (DKN-01) in clinical trials for
260 advanced cancer (NCT01457417, NCT02375880), and was in our study causally linked to higher risk of
261 bone fractures and lower risk of estimated bone mineral density (eBMD). In addition, strong
262 evidence for protective roles of PLGF in CHD, CASP-8 in breast cancer and ST2 in asthma was
263 observed. RAGE was causally linked to several traits, including lower body mass index (BMI) and a
264 corresponding lower risk of type 2 diabetes (T2D), higher total cholesterol and triglycerides and
265 higher risk of prostate cancer and schizophrenia. A small molecule brain penetrant RAGE inhibitor
266 was tested in a phase 2 trial of Alzheimer's disease (NCT00566397), but was stopped early for futility.
267 We saw no strong signal for Alzheimer's disease (or vascular disease) in our MR analysis. Our findings
268 identify potential target-mediated effects across multiple other complex phenotypes that might
269 manifest in beneficial and/or harmful effects on patients receiving RAGE-modifying therapies.

270 We also collated observational evidence for 23 of the 50 protein-trait pairs identified as causal in the
271 MR analysis [supplementary table 10]. The direction of effect inferred from observational studies was
272 concordant with the effect direction from MR estimates for 12 pairs.

273 [Heritability analysis and polygenic risk scores \(PRS\) demonstrates large](#) 274 [differences in genetic architecture.](#)

275 We calculated SNP-heritability contributed by the major reported loci (major loci h_{SNP}^2)
276 [supplementary table 2], as well as additional genome-wide SNP-heritability (polygenic h_{SNP}^2) for each
277 protein included in the SCALLOP CVD-I meta-analysis. We observed a large range of different genetic
278 architectures: Differences in magnitude of the genetic component (h_{SNP}^2) ranged from 0.01 (EGF) to

279 0.46 (IL-6RA). Differences in the contribution from non-genome-wide significant SNPs ranged from
280 essentially monogenic (e.g. IL-6RA) to others showing considerable locus heterogeneity with genetic
281 contributions originating entirely from a polygenic background with no single dominating locus (e.g.
282 PDGF-B and Galanin) [Figure 6B].

283 In addition, we calculated the out of sample variance explained in the independent Malmo Diet and
284 Cancer (MDC) study (N~4,500) both for genome-wide significant loci (major loci V.E._{PRS}), as well as
285 additional variance explained by adding PRS (polygenic V.E._{PRS}) [Figure 6A]. The protein PRS' applied
286 in the MDC study for 11 proteins exceeded 10 % of variance explained (V.E._{PRS}) and the PRS' for
287 another 14 proteins exceeded 5 % of variance explained, suggesting that the genetic contribution to
288 inter-individual variability of CVD-I protein levels is considerable.

289 [A polygenic risk score for circulating ST2 levels shows a dose-response](#) 290 [relationship with asthma.](#)

291 Since circulating ST2 showed strong evidence of causation in asthma and inflammatory bowel disease
292 (IBD) and the polygenic V.E._{PRS} model for ST2 explained nearly 20 % of its variance, we attempted to
293 quantify the effect of the ST2 polygenic V.E._{PRS} on circulating ST2 levels in the MDC study, and risk of
294 asthma and IBD in 337,484 unrelated White British subjects in the UK Biobank. The range of
295 circulating ST2 across 11 categories of the ST2 PRS in MDC was nearly 1.2 standard deviations [Figure
296 7A]. Corroborating the Mendelian randomization analysis, the ST2 PRS showed a strong negative
297 dose-response relationship with risk of asthma ($p=1.2 \times 10^{-8}$) and a positive trend for risk of IBD
298 ($p=0.13$) [Figure 7B and C]. Overlaying the linear trends for ST2 levels, asthma and IBD using meta-
299 regression, an increase in the PRS equivalent to a 1 standard deviation higher circulating ST2,
300 corresponded to a 8.6 % (95%CI 3.8%, 13.2%; $P=0.004$) reduction in the relative risk of asthma and a
301 4.3 % (95%CI -3.8%, 13.0%; $P=0.263$) increase in the relative risk of IBD [Supplementary Figure 8].

302 Reverse Mendelian randomization identifies widespread causal relationships, 303 where complex phenotypes affects CVD-I proteins.

304 To investigate whether genetic susceptibility (liability) to complex disease and phenotypes causally
305 alter circulating levels of CVD-I proteins, we also performed MR using 38 complex phenotypes
306 (including continuous risk factors, such as adiposity and clinical outcomes, such as T2D) as exposure
307 and CVD-I protein levels as outcomes. All CVD-I proteins were causally altered by at least one
308 complex phenotype. BMI and estimated glomerular filtration rate (eGFR) causally affected 32 and 29
309 of the 85 tested proteins respectively [Figure 8A; Supplementary Figure 7C]. BMI seemed to causally
310 affect protein levels in both positive and negative directions, whereas only REN (renin) was causally
311 decreased with genetically higher eGFR. In an effort to elucidate whether these estimates were
312 recapitulated in simple observational analyses, we compared effect estimates from linear regression
313 analyses of associations of BMI and eGFR with each respective CVD-I protein in one of the
314 participating study cohorts (IMPROVE). The correlation between the observational and MR estimates
315 were high for BMI ($R=0.78$), and more modest for eGFR ($R=0.50$) [Figure 8B-C].

316 Discussion

317 Using a meta-analysis approach including >30,000 individuals, we identified and replicated 315
318 primary and 136 secondary pQTLs for 85 circulating proteins to yield new insights for translational
319 studies and drug development. Our study demonstrates that pQTLs can be harnessed to enhance
320 evaluation of therapeutic hypotheses for protein targets, and to support those hypotheses with basic
321 insights into potential protein regulatory pathways and biomarker strategies. However, we also
322 observed large differences between proteins in relation to genetic architecture, suggesting that the
323 relative strength to apply these strategies is likely protein-dependent.

324 Our pQTL-based framework was developed to address several key challenges associated with drug
325 development, including a) mapping of protein regulatory pathways, b) identification of new target

326 candidates c) repositioning of drugs, d) target-associated safety and e) matching of target
327 mechanisms to patients by protein biomarkers or genetic PRS' [Figure 9].

328 The mapping of *trans*-pQTLs, which typically have smaller effects on protein levels [Supplementary
329 Figure 9], was aided by the large SCALLOP discovery sample size, yielding on average 4 independent
330 pQTLs per protein. A causal gene was assigned for each *trans*-pQTL to generate hypotheses that can
331 be further tested using *in vitro* or *in vivo* perturbation experiments. The robustness of causal gene
332 assignments for a few selected *trans*-pQTLs was demonstrated using samples from a randomised
333 controlled trial testing a dual small-molecular inhibitor of the protein products of assigned genes
334 (*CCR5*, *CCR2*) and transgenic mice with liver-specific knockdown of assigned genes (*ABCA1*, *TRIB1*).
335 Although further studies will be needed for orthogonal validation of most of the genes assigned from
336 the CVD-I *trans*-pQTLs, several of the implicated genes have previously been identified as regulators
337 of some of the CVD-I proteins including *CASP1*²⁶, *NLRC4*²⁶ and *GSDMD*²⁷ for IL-18, *FLT1*²⁸ for PLGF,
338 *ADAM17*²⁹ for TNFR1 and *SLC34A1*³⁰ for FGF-23 [Supplementary Table 2].

339 Further, we attempted to estimate the proportion of pQTLs that were likely to be driven by effects
340 on mRNA expression, using multiple eQTL approaches and datasets. The lowest estimate was
341 obtained with SMR/HEIDI, suggesting that 18.4 % of pQTLs were also eQTLs whereas direct look-up
342 and co-localisation analysis using PrediXcan yielded estimates between 26 % - 29 %. We conclude
343 that the majority of pQTLs identified for the CVD-I proteins were not explained by eQTLs.

344 Clinical-stage targeting with any drug modality was reported for 35 of the 90 proteins on the Olink
345 CVD-I panel [Supplementary Table 7]. Our MR analysis identified 11 proteins with causal evidence of
346 involvement in human disease that have not previously been targeted. Among those, four proteins
347 were causal for a disease phenotype and did not show strong evidence of inverse causality with
348 another phenotype (increasing specificity for intended indication), including *CHI3L1* and *SPON1* for
349 atrial fibrillation and *PAPPA* for type-2 diabetes. Strong causal evidence was also identified for
350 proteins targeted in phase-2 or later development. The MR evidence was concordant with drug

351 indications for several protein targets but for some also suggested alternative indications or that
352 monitoring of target-associated safety might be warranted. Monoclonal antibodies that block the
353 CD40 ligand binding to CD40 – a critical element in T cell activation – have been shown to have
354 positive clinical effects in patients with autoimmune diseases; but increased risk of
355 thromboembolism precluded further clinical development³¹. These observations from clinical trials
356 are in line with our findings that genetically *lower* levels of CD40 are associated with *lower* risk of RA,
357 but *higher* risk of stroke. There are ongoing efforts to modify CD40L antibodies to retain efficacy
358 while avoiding thromboembolism³¹. However, our results suggest that decreasing circulating CD40
359 levels may have target-mediated beneficial effects on RA risk, while increasing the risk of ischemic
360 stroke, i.e. that the increased risk of thromboembolism (manifest as stroke) is an on-target adverse
361 effect. TRAIL-R2 is a key receptor for TRAIL, which has been shown to selectively drive tumour cells
362 into apoptosis. Therefore, considerable effort to agonise TRAIL-R2 for treating cancers has been
363 made in the past years³². We demonstrated that increased circulating TRAIL-R2 is protective against
364 prostate cancer, which may suggest that this cancer type should be investigated in clinical trials
365 evaluating the efficacy of TRAIL-R2 agonists.

366 Biomarkers can be broadly classified as generic biomarkers for disease risk or prognosis, or as
367 biomarkers reflecting the activity of specific disease processes or biology. Biomarkers that enable
368 matching of target mechanisms to patient subgroups with greater than average benefit from
369 treatment are enablers of precision medicine. We showed that CCR2/CCR5 small-molecule inhibition
370 modulated circulating levels of CCL-4 and MCP-1, which may suggest that *trans*-pQTLs can guide
371 selection of exploratory biomarkers to monitor the efficacy of target mechanisms. We also identified
372 multiple complex traits causally affecting circulating protein levels. For example, eGFR and BMI
373 causally influenced over 1/3 of the CVD-I proteins, suggesting that future biomarker studies should
374 consider these traits as potential confounders. Moreover, the causal phenotype-to-protein
375 associations may represent pathway-related causality to the complex phenotype of interest; or
376 alternatively, ‘reverse causality’ which might pose an opportunity to evaluate implicated proteins as

377 surrogate biomarkers for efficacy in interventional trials³³. We found that higher BMI causally
378 lowered RAGE, while higher circulating levels of RAGE were causally linked to a lower risk of T2D.
379 Thus, developing a hypothetical therapeutic to increase RAGE might represent a mechanism by
380 which it is possible to off-set the risk of T2D arising from the global increases in obesity.

381 Protein-centric PRS' may allow stratification of individuals with genetic propensity for high circulating
382 protein levels. Only 10 % of the protein-centric PRS' explained 10 % or more of the protein variance
383 in the independent replication cohort, including ST2, a prognostic biomarker for heart failure³⁴. ST2
384 showed evidence of inverse causality in asthma and positive causality in IBD. By constructing a
385 genome-wide polygenic risk score for ST2 levels from the MDC study, applying it to the UK Biobank
386 and comparing asthma and IBD prevalence across eleven quantiles of the ST2 PRS, estimated the
387 magnitude of ST2 increase required to decrease the risk of asthma to similar levels as individuals in
388 the highest ST2 PRS category. Such use of PRS for proteins may be expanded to other disease
389 endpoints and may be of use in precision medicine, to guide which patients may obtain most benefit
390 from drugs that pharmacologically alter individual proteins.

391 In conclusion, our findings provide a comprehensive toolbox for evaluation and exploitation of
392 therapeutic hypothesis and precision medicine approaches in complex disease. Such approaches
393 provide an excellent opportunity to rejuvenate the drug development pipeline for new treatments.

394

395

396

397 **Figure and table legends**

398

399 **Figure 1.** Chromosomal location of all primary associations at conventional GWAS significance of P
400 5×10^{-8} . Cis-pQTLs are shown in red (bold) and trans-pQTLs in blue. The gene annotations refer to the
401 gene closest to the pQTL.

402 **Figure 2.** Classification of cis- and trans-pQTL genes. **A.** The gene ontology label of all cis-pQTL genes,
403 i.e. the protein-encoding genes. **B.** The gene-ontology label of all best-guess trans-pQTL genes. **C.**
404 Gene set enrichment analysis of genes assigned to all significant trans-pQTLs, showing the top-gene
405 sets from the Gene Ontology set Molecular Function.

406 **Figure 3.** Plasma levels of MCP-1 and CCL4 in human subjects treated with a small-molecule dual-
407 inhibitor of CCR5 and CCR2 (PF-04634817) or placebo. Induction of MCP-1 and CCL4 upon
408 inhibition of CCR5 and CCR2 mirrors the observed CVD-I trans-pQTLs.

409 **Figure 4.** Plot showing plasma levels of SCF in *ABCA1* and *TRIB1* transgenic mice compared to wild-
410 type controls. Knockdown of *ABCA1* or *TRIB1* resulted in decreased circulating SCF levels mirroring
411 CVD-I trans-pQTLs for SCF. Shown in the plot are SCF levels of individual mice represented by filled
412 circles (wild-type in blue and transgenic mice in red) and the median level per group.

413 **Figure 5. A.** Heatmap of Mendelian randomization analyses of 38 complex traits. ICD-10 chapter of
414 indication and clinical trial stage indicated for each target **B.** Forest plot showing CVD-I proteins with
415 strong evidence of causality in the Mendelian randomization analysis. Drug development
416 abbreviations: PC: pre-clinical, Ph1: Phase 1, Ph2: Phase 2, Ph3: Phase 3, post-MA: post-marketing
417 authorisation. ICD-10 chapters of disease: A-B: infectious and parasitic; C-D: neoplasms; D: blood and
418 immune; E: endocrine, nutritional and metabolic; F: mental and behavioural; G: nervous system; H:
419 eye, adnexa, ear and mastoid; I: circulatory system; J: respiratory system; K: digestive system; L: skin
420 and subcutaneous tissue; M: musculoskeletal and connective tissue; N: genitourinary; O: pregnancy,
421 childbirth, puerperium; P: perinatal; Q: congenital, deformations and chromosomal; R: clinical and
422 lab findings; S-T: injury, poisoning; U: provisional assignment (new diseases unknown aetiology); V-Y:
423 external causes; Z: health status & health services

424 **Figure 6. A.** SNP-Heritability in the SCALLOP consortium discovery cohorts stratified by contributions
425 major loci (light red) and polygenic effects (dark red). In the independent MDC cohort, additional
426 variability explained by adding major loci (light blue) and polygenic risk scores (dark blue). **B.**
427 Differences in how protein levels are affected by polygenic (non-genome-wide significant) loci vs
428 major loci, shown for both the SCALLOP consortium discovery cohorts as h_{SNP}^2 and for the MDC
429 cohort as variability explained.

430 **Figure 7. A.** Association of a polygenic risk score (PRS) with ST2 levels in the independent MDC
431 cohort. **B.** Association of the ST2 PRS with asthma in the UK-biobank. **C.** Association of the ST2 PRS
432 with inflammatory bowel disease (IBD) in the UK-biobank. The ST2 PRS was divided into 11 quantiles,
433 with the middle group (quantile number 6) as the reference category. Effect estimates are presented
434 as quantile-specific mean differences (ST2) and odds ratios (asthma and IBD) relative to the reference
435 category.

436 **Figure 8. A.** Heatmap showing the causal estimates of 38 complex traits on CVD-I protein levels. **B.**
437 Correlation between beta-values for association between body mass index and circulating levels of
438 CVD-I proteins in the IMPROVE cohort, and causal estimates from the Mendelian randomization
439 analysis of body mass index genetic liability on same CVD-I proteins. **C.** Same as B but for estimated
440 glomerular filtration rate.

441 **Figure 9.** Protein-trait relationships that support target validation, repositioning, target-mediated
442 safety and new candidates for drug development. For more information, see data presented in
443 Supplementary Table 7.

444

445

446 **Supplementary Figure 1.** Chromosomal location of all primary associations that were selected as
447 instrument variables for Mendelian Randomization, i.e. those passing Bonferroni corrected GWAS

448 significance $P < 5.6 \times 10^{-10}$ with replication at nominal $p < 0.05$, or for non-heterogeneous variants
449 ($p < 9 \times 10^{-5}$), surpassing a P -value threshold of $P < 5 \times 10^{-8}$ in the joint discovery and replication meta-
450 analysis.

451

452 **Supplementary Figure 2.** Illustration of the online interactive tools for visualization of genomic loci,
453 regions and plausible networks (www.scallop-consortium.com). **A.** Illustration of hotspot loci on
454 chromosome 10 (left) and illustration of hotspot loci with independent effects established using
455 COJO analysis (right) **B.** Circular Manhattan plot for TNF-R2. **C.** The pathway implicated by trans-
456 pQTLs for plasma TNF-R2. The network shows the likely path from pQTL to TNF-R2.

457 **Supplementary Figure 3.** Heat map showing PrediXcan associations across tissues for any protein
458 with significant associations between protein and predicted mRNA levels ($FDR < 0.05$) in at least one
459 tissue. In each cell, numeric labels correspond to the uncorrected P -value from the association of
460 protein with predicted expression levels. The colour palette shows the relative expression level of the
461 gene across tissues in the GTeX resource.

462 **Supplementary Figure 4.** Effect of exposure to PF-04634817 on EN-RAGE, FGF-23, KIM-1, myoglobin
463 and TNFR-2.

464 **Supplementary Figure 5.** Overview of protein levels having effect on complex phenotypes using
465 Mendelian Randomization. Similar to figure 5B, but also showing effects with intermediate evidence
466 strength.

467 **Supplementary Figure 6.** Overview of complex phenotypes having effect on protein levels using
468 Mendelian Randomization.

469 **Supplementary Figure 7.** Work flows describing meta analysis, decisions on significance and the
470 reasoning behind Mendelian Randomization evidence strength.

471 **Supplementary Figure 8.** Meta-regression of quantiles of ST2 polygenic risk score and relative risk of
472 asthma (left) and inflammatory bowel disease (right). Values plotted on the x-axis relate to
473 the quantile-specific mean difference in ST2 as compared to the 6th quantile. Values plotted on the
474 y-axis relate to the quantile-specific log odds of disease as compared to the 6th quantile. The red line
475 is the slope derived from the meta-regression across the ST2 quantiles of the PRS on log odds of
476 disease, weighted by the standard error of the log odds.

477 **Supplementary Figure 9.** Comparison of absolute effect sizes of all primary cis- and trans loci listed in
478 Supplementary Table 2.

479

480 **Supplementary Table 1.** Information about all measured proteins

481 **Supplementary Table 2.** List of all protein quantitative locus (pQTL) associations

482 **Supplementary Table 3.** Overview of protein-protein interaction (PPI) and text mining (TM) systems
483 biology analysis

484 **Supplementary Table 4.** Systematic analysis of protein quantitative trait loci (pQTL) in previously
485 published literature

486 **Supplementary Table 5.** Investigation of overlap between protein quantitative trait loci (pQTLs) and
487 expression quantitative trait loci (eQTLs)

488 **Supplementary Table 6.** Summary-data-based Mendelian Randomization (SMR) using heterogeneity
489 in dependent instruments (HEIDI) test.

490 **Supplementary Table 7.** Overview of gene products targeted by compounds or antibodies that have
491 been in clinical development

492 **Supplementary Table 8.** Overview of participating cohorts

493 **Supplementary Table 9.** Overview of external genome-wide association study (GWAS) data used in
494 mendelian randomization (MR) analyses

495 **Supplementary Table 10.** Collation of observational evidence from literature and analysis in the
496 IMPROVE cohort

497

498

499

500

501

502

503

504

505

506

507

508

509

510 **URLs**

511 www.scallop-consortium.com

512 www.ebi.ac.uk/gwas/

513 www.proteinatlas.org

514 www.uniprot.org

515 <http://www.pantherdb.org>

516 david.ncicrf.gov

517 clinicaltrials.gov

518 www.ebi.ac.uk/chembl

519 www.drugbank.ca

520 www.opentargets.org

521 neic.no/tryggve/

522 Data availability

523 The full summary statistics of the Olink CVD-I protein GWAS have been deposited at the [SCALLOP-](#)
524 [CVD-I online resource](#), allowing access to interactive SCALLOP-CVD-I tools and unrestricted download
525 access for secondary analyses. Additionally, a full copy has been deposited at
526 <https://doi.org/10.5281/zenodo.2615265> for long-term retention.

527 Online Methods

528 Selection of proteins

529 Proteins for the Olink PEA CVD-I panel were selected by mining the literature for protein biomarkers
530 associated with cardiovascular risk or prognosis in human observational studies and in animal models
531 and by bringing in protein biomarker suggestions from leading cardiovascular disease researchers¹⁰.
532 The list of proteins curated from these sources was then pruned down based on availability of high-
533 quality antibodies and relative abundance of the proteins in human plasma.

534 Intra- and inter-plate coefficients of variation (CV) of the CVD-I panel are available from Olink
535 Proteomics AB (<https://www.olink.com/resources-support/document-download-center/>). In
536 addition, we calculated the inter-plate coefficient of variation using data from a pooled plasma
537 sample in one of the participating cohorts -the IMPROVE study. The mean inter-plate CV was
538 averaged across proteins was 16.6 %, (range 11 % -26 %) [Supplementary Table 1].

539 Cohorts and data collection

540 Summary statistics from GWAS of Olink CVD-I proteins were obtained from 13 cohorts of European
541 ancestry. The details of all study cohorts are shown in [Supplementary Table 9]. Together the cohorts
542 included a total of 21,758 individuals; although the average per-protein sample size was 17,747,
543 since not all proteins passed quality control (QC) in all cohorts. Each cohort provided data imputed to
544 1000 Genomes Project phase 3 reference or later or to the Haplotype Reference Consortium (HRC)
545 reference, which resulted in the testing of 21.4M SNPs. Because imputation schemes varied by
546 cohort, this resulted in an average of 20.3M SNPs under investigation for each protein.

547 Each cohort applied quality control measures for call rate filters, sex mismatch, population outliers,
548 heterozygosity and cryptic relatedness as documented in [Supplementary Table 8]. Prior to running
549 the genetic analyses, NPX values of proteins (on the \log_2 scale) were rank-based inverse normal
550 transformed and/or standardised to unit variance, thus avoiding potential Olink batch-differences
551 between cohorts. Genetic analyses were conducted using additive model regressions, with
552 adjustment for population structure and study-specific parameters [Supplementary Table 8]. Forest
553 plots of cohort-specific effects are available for all significant and suggestive pQTLs using the [online](#)
554 [tool](#). Each contributing cohort uploaded the resulting summary statistics in a standardized format
555 using a secure computational cluster provided by Neic Tryggve (<https://neic.no/tryggve/>). All meta-
556 analysis was performed in duplicate at two different research centres using completely separate
557 bioinformatic pipelines (L.F. and S.G.).

558 Data cleaning and meta-analysis

559 A per-protein filtering threshold of >80% samples above the Olink detection limit was applied to each
560 cohort, leaving data on 90 of the 92 proteins to be analysed. The remaining files had an average of
561 3% missing samples (per cohort statistics available in [Supplementary Table 8]). Minor allele
562 frequencies were compared with those reported in 1000 Genomes EUR. A per-SNP filter was applied
563 based on imputation quality level (at default setting for respective imputation algorithm) and minor

564 allele count (at least 10 alleles per cohort). This resulted in the omission of 10% of the SNPs. Finally,
565 meta-analysis was performed using METAL (2011-03-25)³⁵, applying the inverse-variance weighted
566 approach (i.e. the STDERR option). *Cis*-pQTLs were defined as a signal within 1 Mb of the gene
567 encoding the protein and all other signals were defined as *trans*-pQTLs. See supplementary figure 7A
568 for flow chart overview.

569 Replication analyses

570 We sought to replicate the findings in the Malmö Diet and Cancer (MDC) population-based cohort
571 with 4,678 individuals, and in the Swedish Mammography Cohort Clinical (SMCC, part of the Swedish
572 national research infrastructure SIMPLER described at www.simpler4health.se) population-based
573 study of 4,495 women. In MDC, genotypes were imputed to the Haplotype Reference Consortium
574 reference (HRC Unlimited v1.0.1) and data were analysed using linear regression in EPACTS 3.3.0
575 (linear Wald test). The genotypes in SMCC were measured using Illumina's Global Screening Array
576 and were imputed up to HRC v1.1 and 1000G phase3 (v5), and linear regressions of rank-based
577 inverse-normal transformed protein values adjusting for age, storage time, and PC1-15 were
578 performed using PLINK v2 (4 Mar 2019).

579 Conditional and joint association analysis

580 To identify secondary signals at the 401 loci reported in supplementary table 2, we performed
581 analyses conditioning on the primary signal using conditional-joint analysis in GCTA (version 1.26.0)
582^{36,37}. The Stanley cohort was chosen as an ancestrally well-matched LD-reference cohort. Meta-
583 analysis summary data were processed with filtering for MAF (0.01) and r^2 (<0.001) to ensure that
584 secondary association signals identified were not driven by LD with the primary signal. See
585 supplementary figure 7B for a flow chart of primary and secondary signals.

586 Cross-reference of pQTLs with other complex traits

587 For each pQTL association, we searched PubMed and the EBI GWAS catalogue (URL:
588 <https://www.ebi.ac.uk/gwas/> : November 2018) for published SNPs with any complex trait within
589 10kb or having an LD of $r^2 \geq 0.85$.

590 Comparison between eQTLs and pQTL

591 To identify eQTL that corresponded to each pQTL, we used three independent eQTL studies:
592 LifeLines-DEEP³⁸, GTEx³⁹ and eQTLGen⁴⁰. Each SNP-protein pQTL pair was first converted to SNP-gene
593 pairs using Olink platform protein identification and the gene annotation of Ensembl v91. Then, the
594 significance of eQTLs for these SNP-gene pairs was assessed in three eQTL datasets, using two
595 different cut-offs: a stringent genome-wide significance threshold ($P < 5 \times 10^{-8}$) and a nominal
596 significance of $P < 0.05$.

597 In the eQTL dataset of LifeLines-DEEP, individual-level whole blood RNA-seq, protein and genotype
598 data were available. This allowed for a direct comparison of the concordance of blood eQTLs and
599 pQTLs. To do so, we re-tested eQTL associations for all pQTL pairs, using a previously published
600 pipeline⁴¹. The resulting eQTLs were considered genome-wide significant if it passed the
601 permutation-based FDR < 0.05 level, or to be nominally significant if the P -value was < 0.05 .

602 In the eQTL datasets of GTEx v7 and eQTL-Gen, we did not have access to individual level data. Thus,
603 the comparisons were conducted using publicly available eQTL results. In these datasets, we
604 considered an eQTL genome-wide significant if it was within the reported genome-wide significant
605 list, and nominally significant if it had a nominal P -value < 0.05 . Altogether, if one pQTL pair had at
606 least one significant eQTL effect in any dataset irrespective of allelic direction it was considered an
607 overlapping pQTL-eQTL pair.

608 Expression SMR analysis

609 We performed an SMR and HEIDI (heterogeneity in dependent instruments) analysis¹² to identify the

610 expression levels of genes that were associated with protein abundance through pleiotropy using
611 pQTL summary statistics from this study and cis-eQTL summary data from published studies^{42,43}.

612 The eQTL summary data used in the SMR analysis were from the Consortium for the Architecture of
613 Gene Expression (CAGE), comprising 38,624 normalized gene expression probes and ~8 million SNPs
614 from 2,765 blood samples. The eQTL effects were in standard deviation (SD) units of expression
615 levels. We excluded the gene probes in the major histocompatibility complex (MHC) region and
616 included only the gene probes with at least one cis-eQTL at $P < 5 \times 10^{-8}$ (a basic assumption of SMR),
617 resulting in 9,538 gene expression probes.

618 The SMR test uses a SNP instrument (i.e., the top associated eQTL) to detect association between
619 two phenotypes (i.e., gene and protein in this case). The HEIDI test utilises LD between the SNP
620 instrument and other SNPs in the cis-region to distinguish whether the association identified by the
621 SMR test is driven by a set of shared genetic variants between two traits (pleiotropic or causal model)
622 or distinct sets of variants in LD (linkage model)¹². Only the associations that surpassed the genome-
623 wide significance level of the SMR test ($P_{\text{SMR}} < 0.05 / m$ with m being the number of SMR tests) and
624 were not rejected by the HEIDI test ($P_{\text{HEIDI}} > 0.01$) were reported as significant.

625 [PrediXcan and transcript-wide association of CVD-I protein levels](#)

626 Imputation of gene expression was performed in the IMPROVE study. After standard quality control,
627 genotypes were pre-phased using Eagle2, and then subsequently imputed by minimac4 using the
628 1000 Genomes reference. A filter on RSQ 0.8 and minor allele frequency 0.01 was set on the imputed
629 genotypes prior to prediction with PrediXcan, which used 44 tissue models based on GTEx v7.

630 Using protein data collected on the CVD-I chip in the same individuals, the associations between
631 protein levels in plasma and the predicted expression of their respective coding gene across 20
632 tissues (from the PrediXcan model) were modelled by a linear model in R. False discovery rate were
633 estimated based on Q-values (using the R package qvalue). In total, 64 genes in one to 18 tissues

634 were tested for associations between protein levels and predicted expression. Heatmaps were
635 constructed (using the pheatmap package in R) for any gene with a significant association (FDR<0.05)
636 in at least one tissue.

637 Systems Biology

638 Two sets of network analysis were performed, one using the protein-protein interaction (PPI) data
639 from the inBio Map™ (InWeb_InBioMap) and one using significant associations from text-mining
640 (TM). These two networks each had 13,033 and 14,635 nodes, respectively; and 147,882 and 193,777
641 edges, respectively. In both setups, the shortest path between any of the cis-gene intermediaries to
642 the protein was identified; altogether 10,222 pairs were compared. Of the 372 trans-pQTL
643 associations reported in [Supplementary Table 2], 335 associations had both cis-gene intermediaries
644 and plasma protein in the network allowing their analysis. The likelihood of a path arising by chance
645 was calculated by permutation sampling, using 1,000,000 random networks were generated with a
646 conserved degree distribution. A new algorithm was developed for *de novo* random network
647 generation, which generated random networks with a nearly conserved degree distribution in a
648 feasible time-frame. Further details are available in [Supplementary Notes 1].

649 Assignment of cis-intermediary genes

650 To assign the most plausible causal gene for each of the CVD-I trans-pQTLs we applied a hierarchical
651 approach based on analysis of InWeb_InBioMap PPI, TM, and genomic distance between gene and
652 lead variant at each locus. Results were then manually reviewed by literature, gene expression
653 analysis (proteinatlas.org) and published pQTLs which led to the re-assignment of 52 genes. The
654 algorithmic gene assignment was overruled or complemented for instances when the assigned gene
655 was different from the gene assigned by multiple prior studies [Supplementary table 4]. Gene
656 Ontology analysis of most plausible genes was performed using the DAVID bioinformatics tools and
657 the GO MF gene set definition, with default settings. The Panther pathway tool, Uniprot and the
658 Human Protein Atlas were used to classify the genes according to basic functional class (see URLs).

659 Human in-vivo validation of trans-pQTLs

660 PF-04634817 is a competitive dual inhibitor of CCR2 and CCR5 receptors. In the recent B1261007
661 study, (ClinicalTrials.gov Identifier: NCT01712061), samples were collected from subjects with
662 diabetic nephropathy and treated with PF-04634817 for 12 weeks. CCL-2 (MCP-1) was measured in
663 serum by ELISA at Eurofins (The Netherlands). CCL4 (MIP-1b) and CCL-8 were measured in plasma
664 using Luminex assays (Bio-Rad, Berkeley, CA). CCL5 (RANTES), was measured in plasma as part of a
665 multi-analyte panel at Myriad Rules Based Medicine (Austin, TX).

666 Mouse in-vivo validation of trans-pQTLs

667 Plasma from transgenic- and matched control mice were randomised on a PCR plate. The samples
668 included five mice with targeted deletion of hepatocyte ABCA1²¹ together with five matched control
669 mice, three mice with whole-body TRIB1²² knockdown and three controls and four mice with liver-
670 specific knockdown of TRIB1 and four matched controls. Protein levels of stem cell factor (SCF) was
671 measured using the Olink PEA Mouse exploratory panel according to the manufacturer's instruction
672 (Olink Proteomics, Uppsala, Sweden). The plasma levels of SCF were normalised against average
673 protein concentrations using information on an additional 91 proteins. TRIB1 whole-body and liver-
674 specific mice were analysed jointly as were the respective wild-type controls. The median plasma
675 levels of SCF were compared using the Mann-Whitney U test for unpaired samples.

676 Mendelian Randomization

677 To study the causal effects of the protein on selected disease outcomes, we performed two-sample
678 Mendelian randomization analyses. We used between-study heterogeneity to guide the instrumental
679 variable selection. In the presence of between-study heterogeneity ($P\text{-het} < 9 \times 10^{-5}$), variants had to
680 surpass a Bonferroni-corrected p-value threshold in discovery ($P < 5.6 \times 10^{-10}$) and show nominal
681 significance ($P < 0.05$) in the replication studies (9,173 individuals), with directionally concordant beta
682 coefficients. In the absence of between-study heterogeneity we included variants showing
683 conventional genome-wide significance ($P < 5 \times 10^{-8}$) in a meta-analysis of the discovery and replication

684 datasets. From these, we created two sets of instrumental variables (IVs) for each of the 85 proteins
685 with variants reaching multiple testing-corrected significance in our discovery GWAS: (a) *cis* IVs
686 including one or more independent variants (LD $r^2=0.001$ within $\pm 1\text{Mb}$ of the transcript boundaries of
687 the gene encoding the protein); and (b) *pan* IVs including all independent (LD $r^2=0$) variants
688 associated with the protein, i.e. combining *cis* and *trans* pQTLs. The per-allelic beta coefficients from
689 the main GWAS analyses were used as weights in the IVs. For the outcomes, we obtained the
690 relevant SNP-to-trait summary statistics from publicly-available GWAS as outcomes [Supplementary
691 Table 9]. When lead variants from our main GWAS were not available in these summary statistics, we
692 replaced them with proxies (LD $r^2>0.85$). For each individual SNP-protein and SNP-outcome
693 association, we generated an instrumental variable Wald ratio estimate, with standard errors
694 obtained using the delta method. When the instrument included more than one SNP, summary IV
695 estimates were generated by combining individual SNP Wald estimates by inverse-variance weighted
696 fixed-effect meta-analysis. We report associations with a Benjamini-Hochberg false discovery rate
697 (FDR) $\leq 5\%$, applied separately to summary estimates from *cis*-pQTL and *pan*-pQTL IVs, using pooled
698 estimates for all 38 diseases. We graded the evidence of causality using a framework outlined in
699 [Supplementary Figure 7], using the following categories: strong (*cis*-IV estimate FDR $\leq 5\%$);
700 intermediate (*pan*-IV estimate FDR $\leq 5\%$ with: (i) no heterogeneity between *cis*-IV estimate and *pan*-
701 IV estimate; *and* (ii) no evidence of the MR estimate being unduly influenced by a *trans*-pQTL in
702 leave-one-out analysis); or weak (*pan*-IV estimate FDR $\leq 5\%$ but: no *cis*-pQTL IV available;
703 heterogeneity between *cis*- and all- IVs; or evidence of undue influence by a *trans*-pQTL).
704 Heterogeneity between *pan*-IV and *cis*-IV estimates were calculated using Cochran's Q tests, with
705 $P<0.05$ denoting evidence against the null hypothesis, and applying a Bonferroni adjustment for
706 multiple testing. Mendelian randomization was conducted in duplicate by two separate analysts and
707 analyses were performed in Stata (StataCorp, Texas, USA) version 13.3 using the *mrivests*, *metan* and
708 *multproc* commands and R. Of the 2437 IV estimates derived using *cis*-pQTL instruments across the
709 85 proteins and 38 outcome traits, the IV estimates of 50 protein-to-disease associations met the

710 FDR \leq 5% (corresponding to an uncorrected $P\leq 1.1\times 10^{-3}$). Of the 3044 IV estimates composed using all
711 pQTL instruments, 281 IV estimates met FDR \leq 5% (corresponding to $P\leq 4.7\times 10^{-3}$; [Figure 5A]. The
712 decision tree for scoring the strength of MR evidence is available in [Supplementary Figure 7].

713 Heritability analyses

714 We estimated the total SNP-heritability (h_{SNP}^2) for the plasma level of each protein from the summary
715 statistics of each individual GWAS by summing the contributions from two independent partitions of
716 the SNPs: primary major loci and polygenic background. We defined the variance explained by
717 primary major loci (major loci h_{SNP}^2) as the sum of the estimated variance explained ($2*\beta^2*f*(1-f)$),
718 where f is the minor allele frequency, and owing to the fact that the phenotypic variance has been
719 standardized across lead SNPs indexing all primary genome-wide significant loci. We used LDSC
720 regression⁴⁴ to estimate the contribution of the polygenic background (polygenic h_{SNP}^2) for each
721 protein, which we define as the contribution of all loci not indexed by a genome-wide significant lead
722 SNP. LDSC regression is known to perform poorly when large effect, major genes are present, as it
723 was derived under the assumption of a simple polygenic genetic architecture⁴⁴. To account for this
724 and avoid double counting the variance explained by major loci through LD surrogates, prior to
725 estimating the LDSC regression polygenic h_{SNP}^2 , we censored all SNPs within 10 Mb of genome-wide
726 significant lead SNPs for all primary loci.

727 Polygenic risk score calculation

728 Polygenic risk scores were derived using LDpred algorithm⁴⁵, which adjusts the effect of each SNP
729 allele for those of other SNP alleles in linkage disequilibrium (LD) with it, and also takes into account
730 the likelihood of a given allele to have a true effect according to a user-defined parameter, which we
731 used as all 7 default LDpred-settings, with values from 1 through 1×10^{-5} . The algorithm was directed
732 to use HapMap3 SNPs that had a minor allele frequency >0.05 , Hardy-Weinberg equilibrium $P>1e-05$
733 and genotype-yield >0.95 , consistent. Variance explained in the independent MDC-study was tested
734 according to a step-wise model, first including non-genetic covariates, then additional variability

735 explained by adding SNPs from genome-wide significant SNPs (major loci V.E._{PRS}), and then additional
736 variability explained by adding the 7 LDpred-derived scores as additional covariates (polygenic
737 V.E._{PRS}).

738 ST2 polygenic risk score for asthma and inflammatory bowel disease in the UK 739 biobank

740 Prior to analysis subjects who were not White British (based on self-reported ancestry in
741 combination with genetic PCA) in the maximum unrelated subset were filtered out. All bi-allelic SNPs
742 with MAF \geq 1% and MaCH rsq \geq 0.8 were kept. The Z-score transformed LDpred PRS (wt2) for ST2
743 was calculated as described for MDC in 337,484 White British UK Biobank participants. Association
744 with asthma and IBD were tested using logistic regression adjusting for age, sex, PC1-10, genotype
745 batch using either the continuous PRS or the PRS quantile-bins as predictors. The UK Biobank
746 protocol has been described previously⁴⁶ and is available online (<https://www.ukbiobank.ac.uk>). The
747 genotype quality control (QC), phasing, and imputation was performed centrally and has been
748 previously described⁴⁷. Outcomes (defined based on self-reported data at baseline and/or the
749 inpatient and death registry [including primary and secondary causes as well as prevalent and
750 incident disease]) Asthma: Self-reported touchscreen (6152), self-reported nurse interview (20002),
751 or ICD-10 "J45". Conflicting self-reported results set to missing unless "J45" was reported.
752 Inflammatory bowel disease: nurse interview (20002) or ICD-10 K50-K52.

753 Meta-regression analysis for ST2 PRS, asthma and IBD

754 We estimated the per-quantile and per-SD associations of the weighted PRS for ST2 (MDC study) on
755 risks of asthma and IBD (UK Biobank) by taking the quantile associations with ST2, asthma and IBD
756 and conducting meta-regression analyses whereby the dependent variable was the quantile-specific
757 logOR and corresponding SE of asthma or IBD and the independent variable was the quantile specific
758 beta coefficient for ST2. This was conducted using the "metareg" package in STATA SE v13.1
759 (Statacorp, USA). Plots from the metaregression are presented in [Supplementary Figure 8].

760 Observational evidence

761 Observational evidence for the CVD-I proteins showing strong evidence of causality in Mendelian
762 randomization was collated from literature or by de-novo analysis in the IMPROVE cohort
763 [supplementary table 10]. To identify evidence from literature, we searched for the protein name or
764 aliases in combination with the implicated trait trait/disease in PubMed. For clinical outcome traits,
765 only those reported as “significant” by the paper were included, and the table provides the
766 directional information provided. For quantitative outcome traits, standardised betas and p-values
767 are reported.

768

769

770

771

772

773

774

775

776

777

778

779

780

781

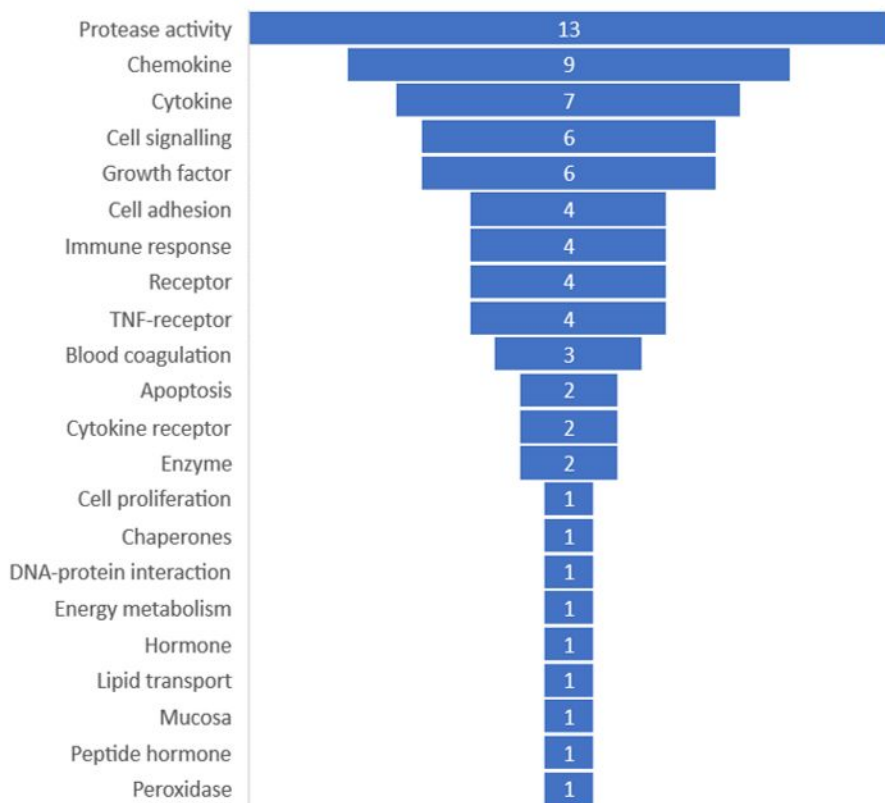
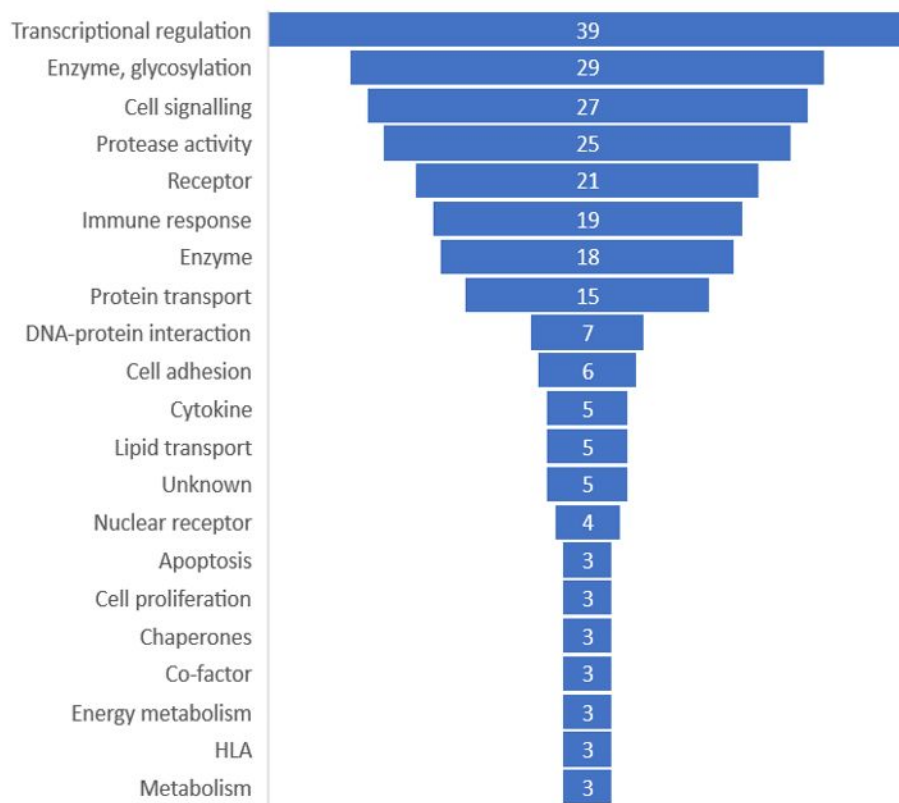
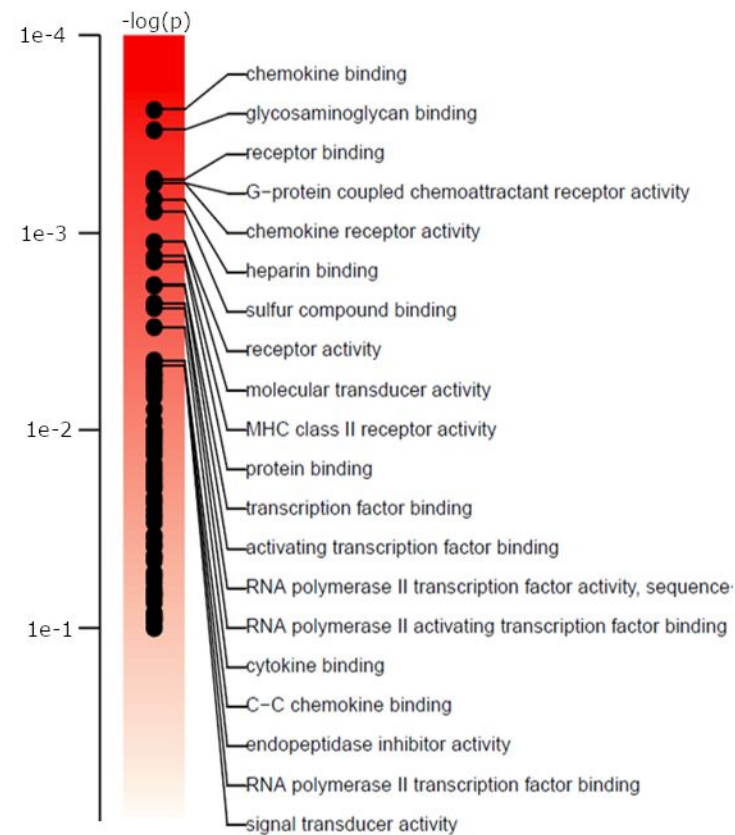
782 References

- 783 1. Chames, P., Van Regenmortel, M., Weiss, E. & Baty, D. Therapeutic antibodies: successes,
784 limitations and hopes for the future. *Br J Pharmacol* **157**, 220-233 (2009).
- 785 2. Holmes, M.V., Ala-Korpela, M. & Smith, G.D. Mendelian randomization in cardiometabolic
786 disease: challenges in evaluating causality. *Nat Rev Cardiol* **14**, 577-590 (2017).
- 787 3. Folkersen, L., *et al.* Mapping of 79 loci for 83 plasma protein biomarkers in cardiovascular
788 disease. *PLoS Genet* **13**, e1006706 (2017).

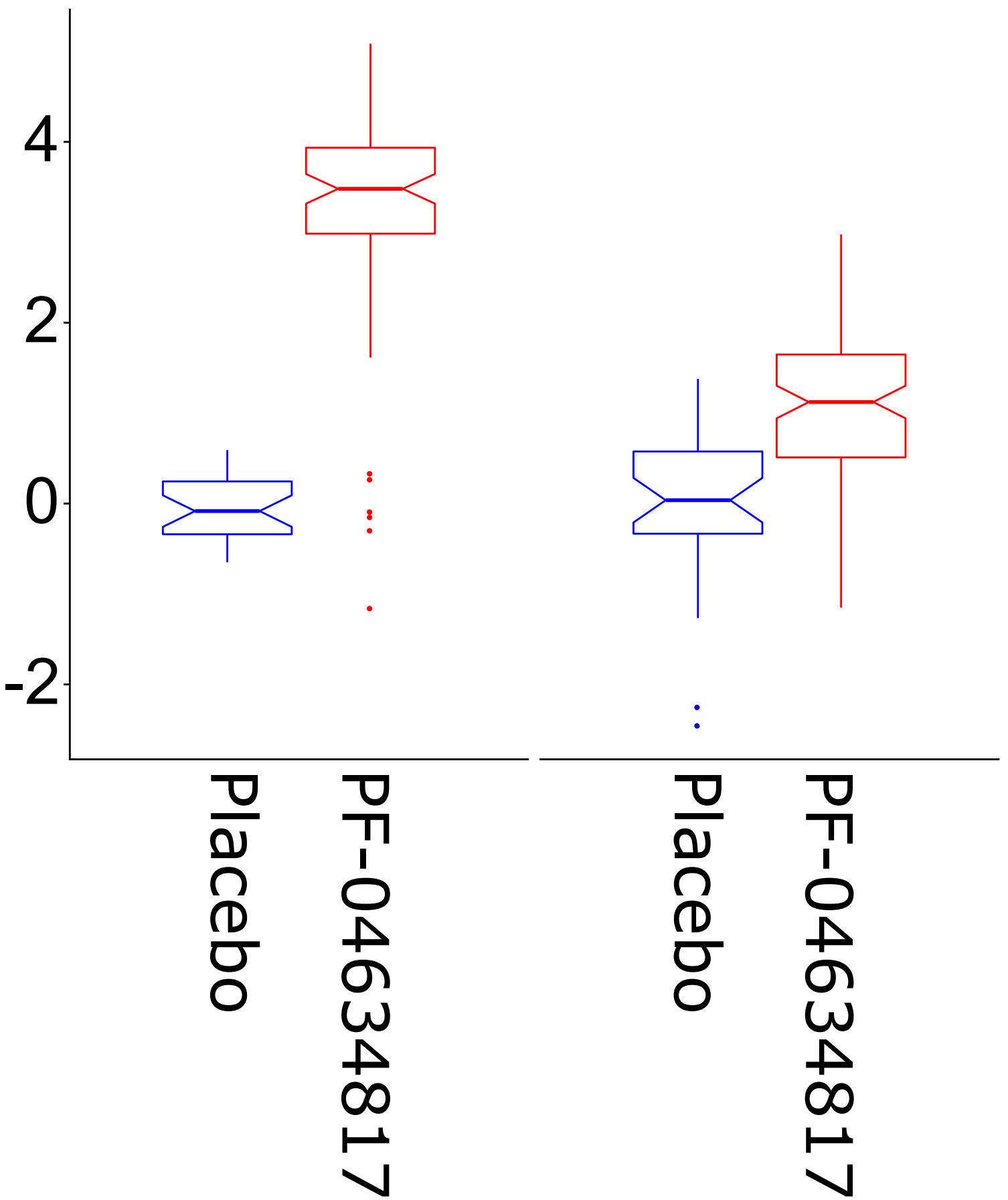
- 789 4. Sun, B.B., *et al.* Genomic atlas of the human plasma proteome. *Nature* **558**, 73-79 (2018).
- 790 5. Williams, S.A., *et al.* Plasma protein patterns as comprehensive indicators of health. *Nat Med*
791 **25**, 1851-1857 (2019).
- 792 6. Lehallier, B., *et al.* Undulating changes in human plasma proteome profiles across the
793 lifespan. *Nat Med* **25**, 1843-1850 (2019).
- 794 7. Enroth, S., Johansson, A., Enroth, S.B. & Gyllenstein, U. Strong effects of genetic and lifestyle
795 factors on biomarker variation and use of personalized cutoffs. *Nat Commun* **5**, 4684 (2014).
- 796 8. Emilsson, V., *et al.* Co-regulatory networks of human serum proteins link genetics to disease.
797 *Science* **361**, 769-773 (2018).
- 798 9. Melzer, D., *et al.* A genome-wide association study identifies protein quantitative trait loci
799 (pQTLs). *PLoS Genet* **4**, e1000072 (2008).
- 800 10. Assarsson, E., *et al.* Homogenous 96-plex PEA immunoassay exhibiting high sensitivity,
801 specificity, and excellent scalability. *PLoS One* **9**, e95192 (2014).
- 802 11. Gamazon, E.R., *et al.* A gene-based association method for mapping traits using reference
803 transcriptome data. *Nat Genet* **47**, 1091-1098 (2015).
- 804 12. Zhu, Z., *et al.* Integration of summary data from GWAS and eQTL studies predicts complex
805 trait gene targets. *Nat Genet* **48**, 481-487 (2016).
- 806 13. Sun, W., *et al.* Common Genetic Polymorphisms Influence Blood Biomarker Measurements in
807 COPD. *PLoS Genet* **12**, e1006011 (2016).
- 808 14. Chick, J.M., *et al.* Defining the consequences of genetic variation on a proteome-wide scale.
809 *Nature* **534**, 500-505 (2016).
- 810 15. Zhernakova, D.V., *et al.* Individual variations in cardiovascular-disease-related protein levels
811 are driven by genetics and gut microbiome. *Nat Genet* **50**, 1524-1532 (2018).
- 812 16. Solomon, T., *et al.* Identification of Common and Rare Genetic Variation Associated With
813 Plasma Protein Levels Using Whole-Exome Sequencing and Mass Spectrometry. *Circ Genom*
814 *Precis Med* **11**, e002170 (2018).
- 815 17. Cabre, A., *et al.* Fatty acid binding protein 4 is increased in metabolic syndrome and with
816 thiazolidinedione treatment in diabetic patients. *Atherosclerosis* **195**, e150-158 (2007).
- 817 18. Nishimoto, N., *et al.* Mechanisms and pathologic significances in increase in serum
818 interleukin-6 (IL-6) and soluble IL-6 receptor after administration of an anti-IL-6 receptor
819 antibody, tocilizumab, in patients with rheumatoid arthritis and Castleman disease. *Blood*
820 **112**, 3959-3964 (2008).
- 821 19. Gustot, T., *et al.* Profile of soluble cytokine receptors in Crohn's disease. *Gut* **54**, 488-495
822 (2005).
- 823 20. Gale, J.D., *et al.* Effect of PF-04634817, an Oral CCR2/5 Chemokine Receptor Antagonist, on
824 Albuminuria in Adults with Overt Diabetic Nephropathy. *Kidney Int Rep* **3**, 1316-1327 (2018).
- 825 21. Bashore, A.C., *et al.* Targeted Deletion of Hepatocyte Abca1 Increases Plasma HDL (High-
826 Density Lipoprotein) Reverse Cholesterol Transport via the LDL (Low-Density Lipoprotein)
827 Receptor. *Arterioscler Thromb Vasc Biol* **39**, 1747-1761 (2019).
- 828 22. Burkhardt, R., *et al.* Trib1 is a lipid- and myocardial infarction-associated gene that regulates
829 hepatic lipogenesis and VLDL production in mice. *J Clin Invest* **120**, 4410-4414 (2010).
- 830 23. Rosa, M., *et al.* A Mendelian randomization study of IL6 signaling in cardiovascular diseases,
831 immune-related disorders and longevity. *NPJ Genom Med* **4**, 23 (2019).
- 832 24. Interleukin 1 Genetics, C. Cardiometabolic effects of genetic upregulation of the interleukin 1
833 receptor antagonist: a Mendelian randomisation analysis. *Lancet Diabetes Endocrinol* **3**, 243-
834 253 (2015).
- 835 25. Mahdessian, H., *et al.* Integrative studies implicate matrix metalloproteinase-12 as a culprit
836 gene for large-artery atherosclerotic stroke. *J Intern Med* **282**, 429-444 (2017).
- 837 26. Kaplanski, G. Interleukin-18: Biological properties and role in disease pathogenesis. *Immunol*
838 *Rev* **281**, 138-153 (2018).
- 839 27. Heilig, R., *et al.* The Gasdermin-D pore acts as a conduit for IL-1beta secretion in mice. *Eur J*
840 *Immunol* **48**, 584-592 (2018).

- 841 28. Autiero, M., *et al.* Role of PlGF in the intra- and intermolecular cross talk between the VEGF
842 receptors Flt1 and Flk1. *Nat Med* **9**, 936-943 (2003).
- 843 29. Dri, P., *et al.* TNF-Induced shedding of TNF receptors in human polymorphonuclear
844 leukocytes: role of the 55-kDa TNF receptor and involvement of a membrane-bound and
845 non-matrix metalloproteinase. *J Immunol* **165**, 2165-2172 (2000).
- 846 30. Tenenhouse, H.S. & Sabbagh, Y. Novel phosphate-regulating genes in the pathogenesis of
847 renal phosphate wasting disorders. *Pflugers Arch* **444**, 317-326 (2002).
- 848 31. Xie, J.H., *et al.* Engineering of a novel anti-CD40L domain antibody for treatment of
849 autoimmune diseases. *J Immunol* **192**, 4083-4092 (2014).
- 850 32. de Miguel, D., Lemke, J., Anel, A., Walczak, H. & Martinez-Lostao, L. Onto better TRAILs for
851 cancer treatment. *Cell Death Differ* **23**, 733-747 (2016).
- 852 33. Holmes, M.V. & Davey Smith, G. Can Mendelian Randomization Shift into Reverse Gear? *Clin*
853 *Chem* **65**, 363-366 (2019).
- 854 34. McCarthy, C.P. & Januzzi, J.L., Jr. Soluble ST2 in Heart Failure. *Heart Fail Clin* **14**, 41-48 (2018).
- 855 35. Willer, C.J., Li, Y. & Abecasis, G.R. METAL: fast and efficient meta-analysis of genomewide
856 association scans. *Bioinformatics* **26**, 2190-2191 (2010).
- 857 36. Yang, J., Lee, S.H., Goddard, M.E. & Visscher, P.M. GCTA: a tool for genome-wide complex
858 trait analysis. *Am J Hum Genet* **88**, 76-82 (2011).
- 859 37. Yang, J., *et al.* Conditional and joint multiple-SNP analysis of GWAS summary statistics
860 identifies additional variants influencing complex traits. *Nat Genet* **44**, 369-375, S361-363
861 (2012).
- 862 38. Tigchelaar, E.F., *et al.* Cohort profile: LifeLines DEEP, a prospective, general population cohort
863 study in the northern Netherlands: study design and baseline characteristics. *BMJ Open* **5**,
864 e006772 (2015).
- 865 39. Consortium, G.T., *et al.* Genetic effects on gene expression across human tissues. *Nature* **550**,
866 204-213 (2017).
- 867 40. Urmo Vösa, e.a. Unraveling the polygenic architecture of complex traits using blood eQTL
868 metaanalysis. *bioRxiv* **October 19**(2018).
- 869 41. Westra, H.J., *et al.* Systematic identification of trans eQTLs as putative drivers of known
870 disease associations. *Nat Genet* **45**, 1238-1243 (2013).
- 871 42. Lloyd-Jones, L.R., *et al.* The Genetic Architecture of Gene Expression in Peripheral Blood. *Am*
872 *J Hum Genet* **100**, 371 (2017).
- 873 43. McRae, A.F., *et al.* Identification of 55,000 Replicated DNA Methylation QTL and Their Role in
874 Disease. *bioRxiv* **166710**(2017).
- 875 44. Bulik-Sullivan, B.K., *et al.* LD Score regression distinguishes confounding from polygenicity in
876 genome-wide association studies. *Nat Genet* **47**, 291-295 (2015).
- 877 45. Vilhjalmsón, B.J., *et al.* Modeling Linkage Disequilibrium Increases Accuracy of Polygenic Risk
878 Scores. *Am J Hum Genet* **97**, 576-592 (2015).
- 879 46. Sudlow, C., *et al.* UK biobank: an open access resource for identifying the causes of a wide
880 range of complex diseases of middle and old age. *PLoS Med* **12**, e1001779 (2015).
- 881 47. Bycroft, C., *et al.* The UK Biobank resource with deep phenotyping and genomic data. *Nature*
882 **562**, 203-209 (2018).

883

(A) Cis-pQTL genes**(B) Trans-pQTL genes****(C) Trans-pQTL genes, enrichment**

Log2(fold-change)

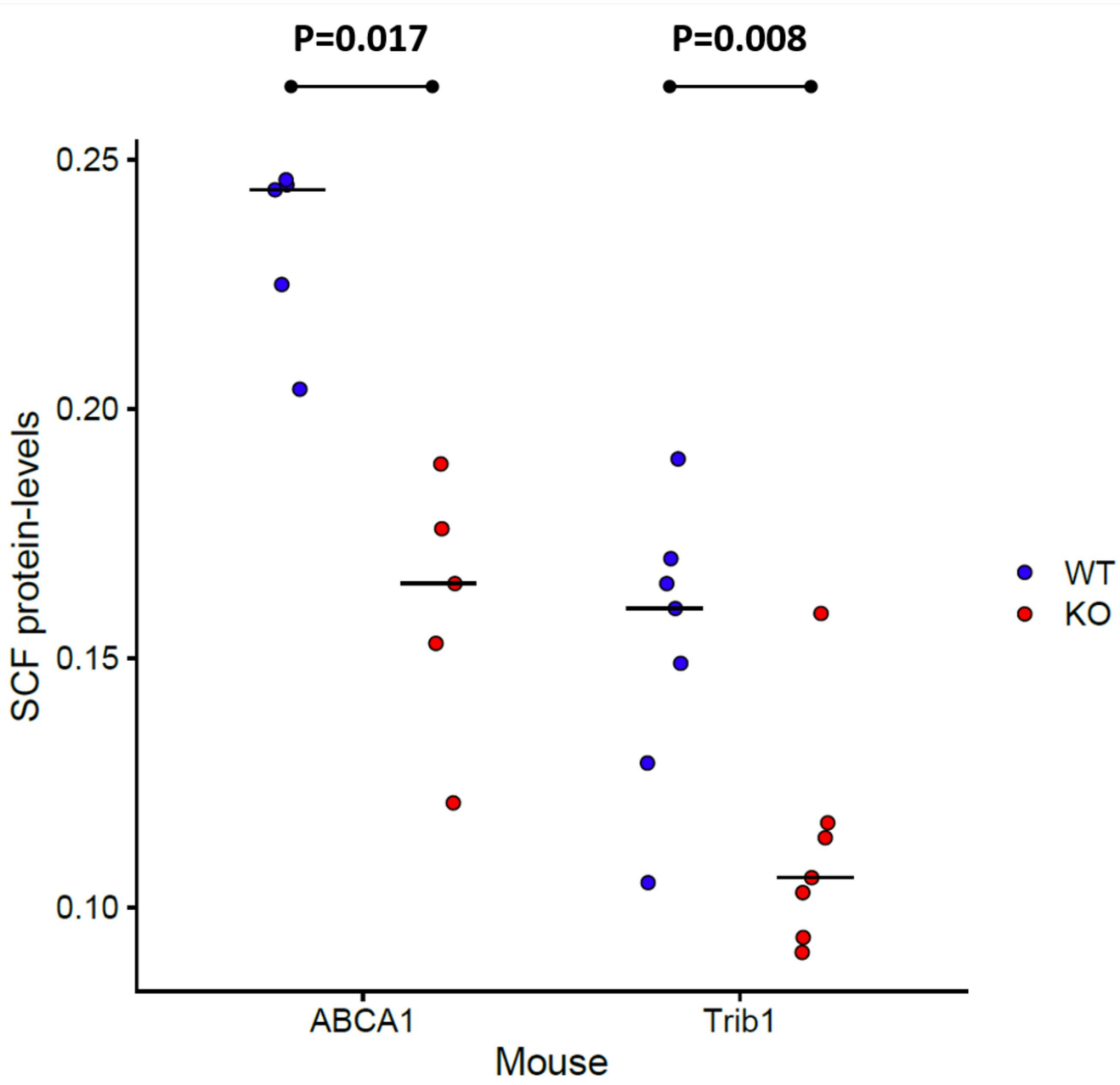


MCP-1

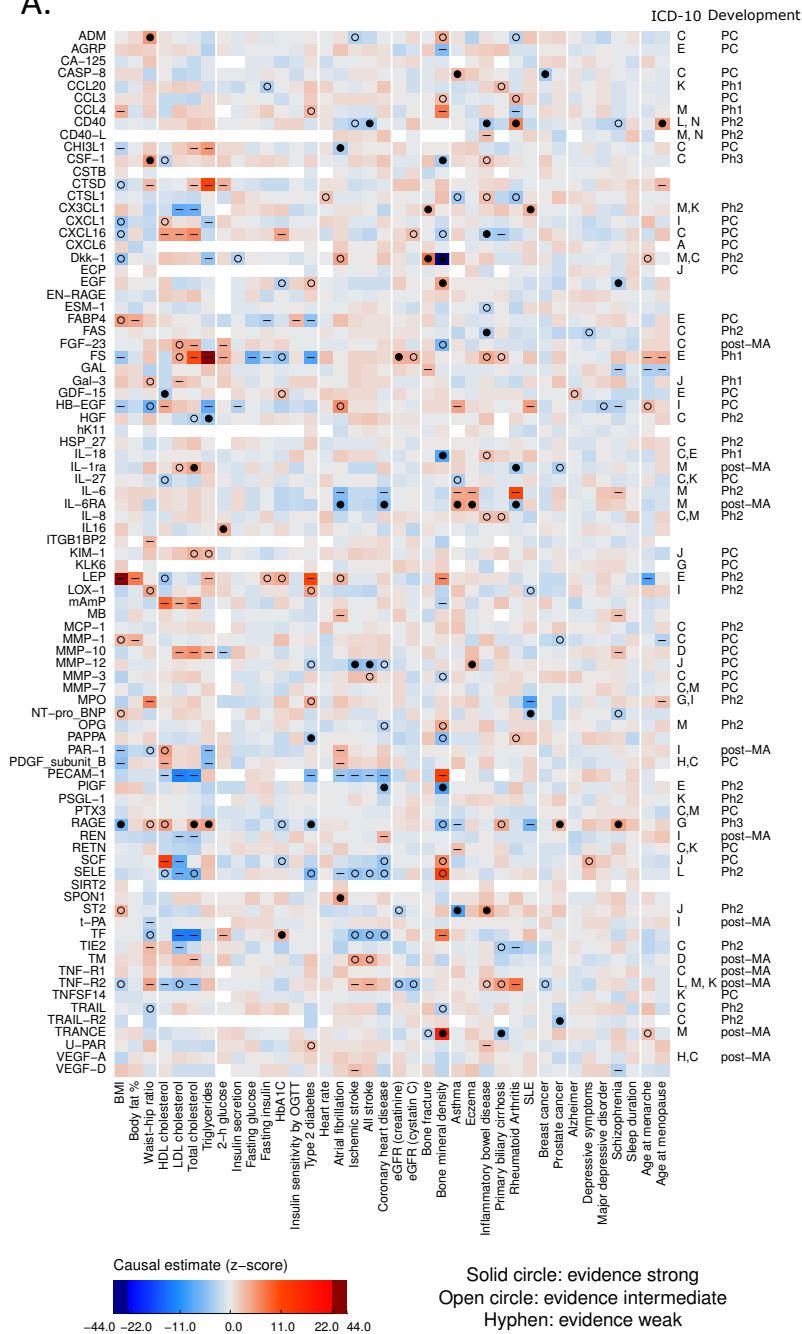
CCL4

Placebo
PF-04634817

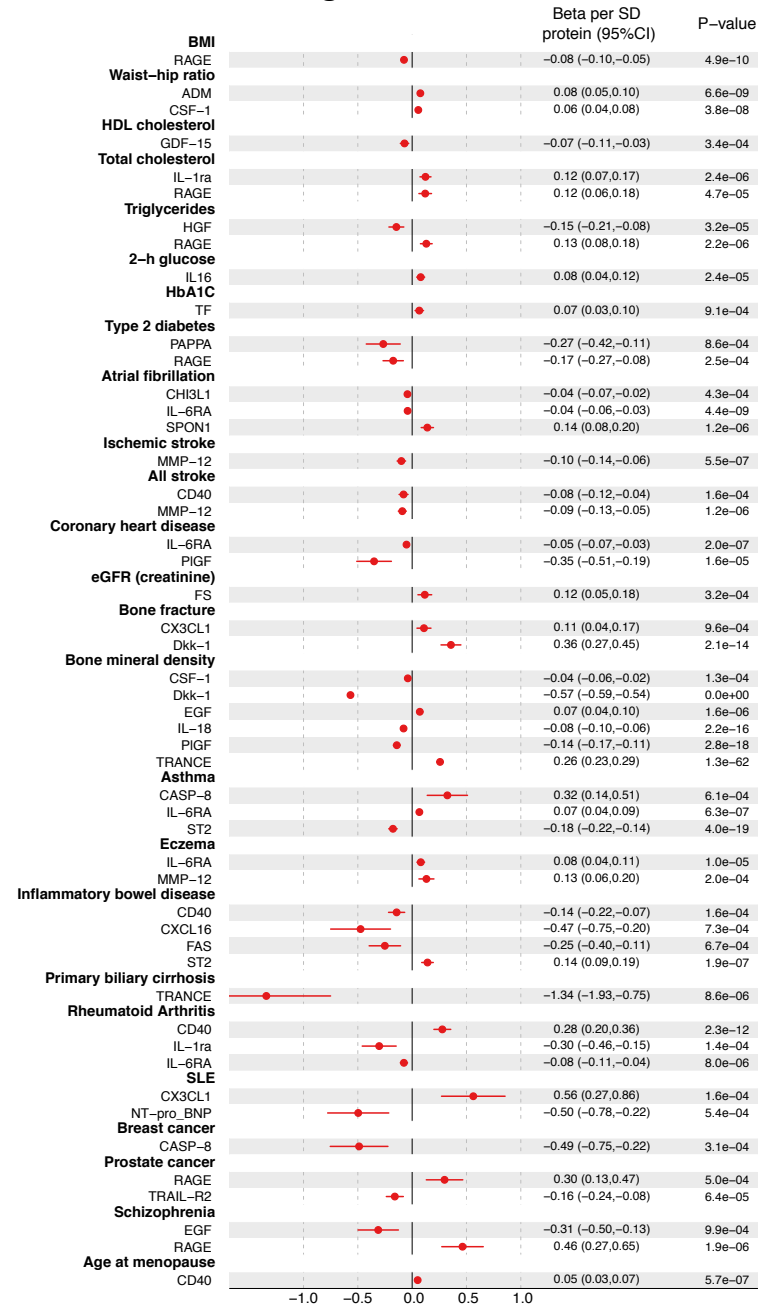
Placebo
PF-04634817

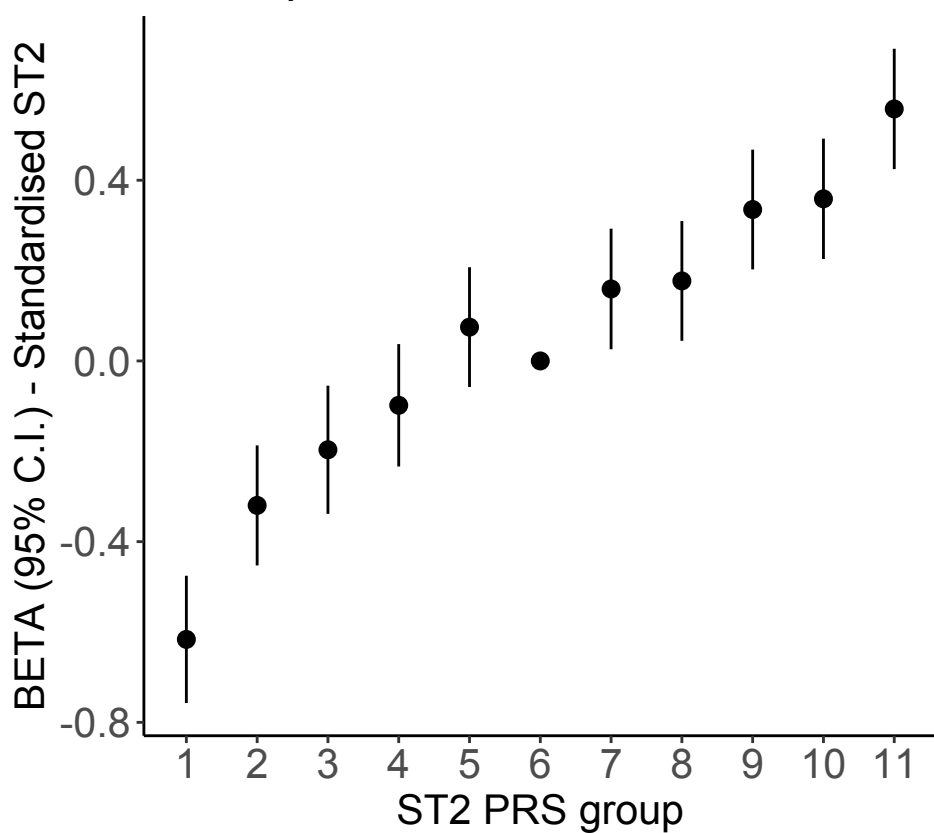
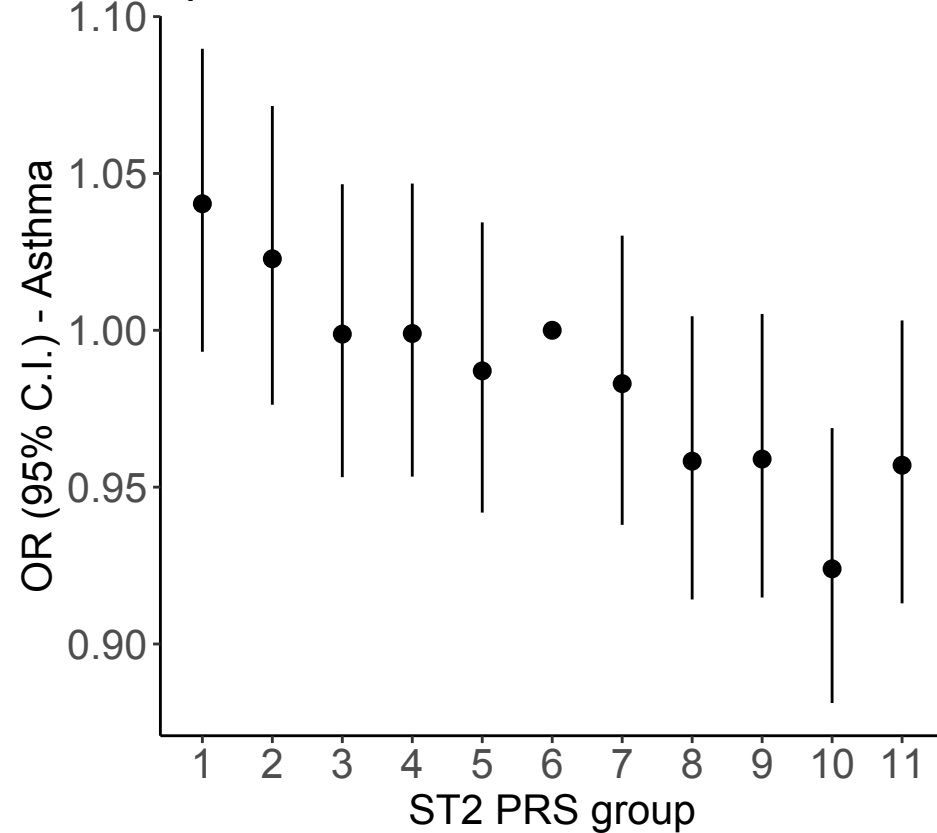
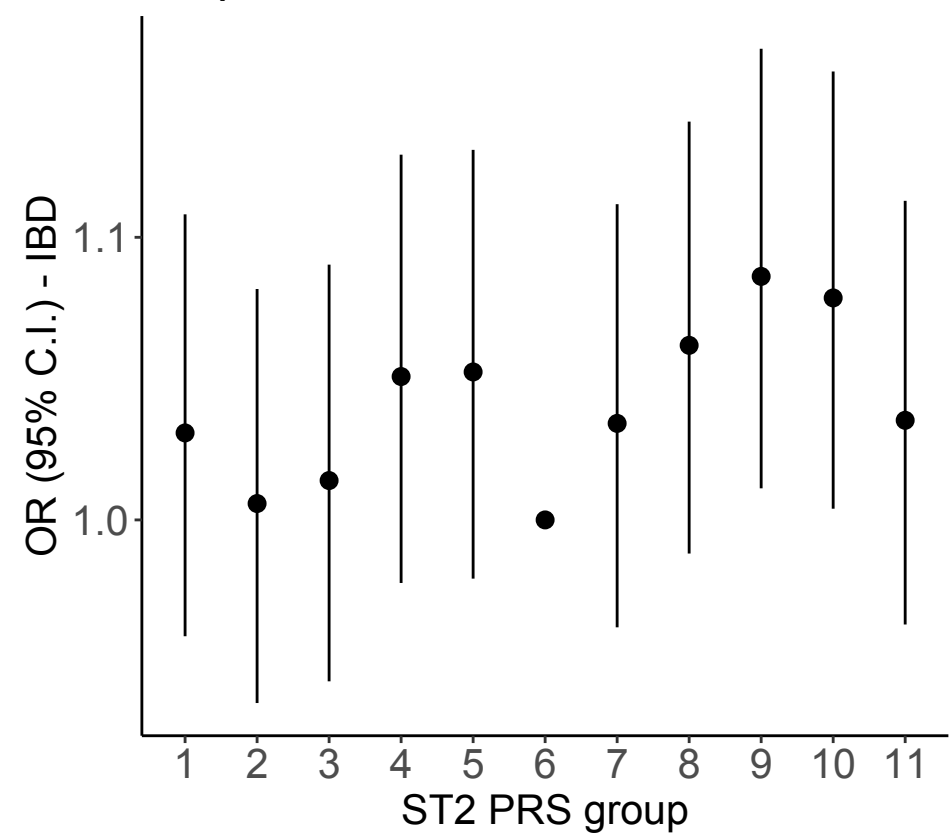


A.

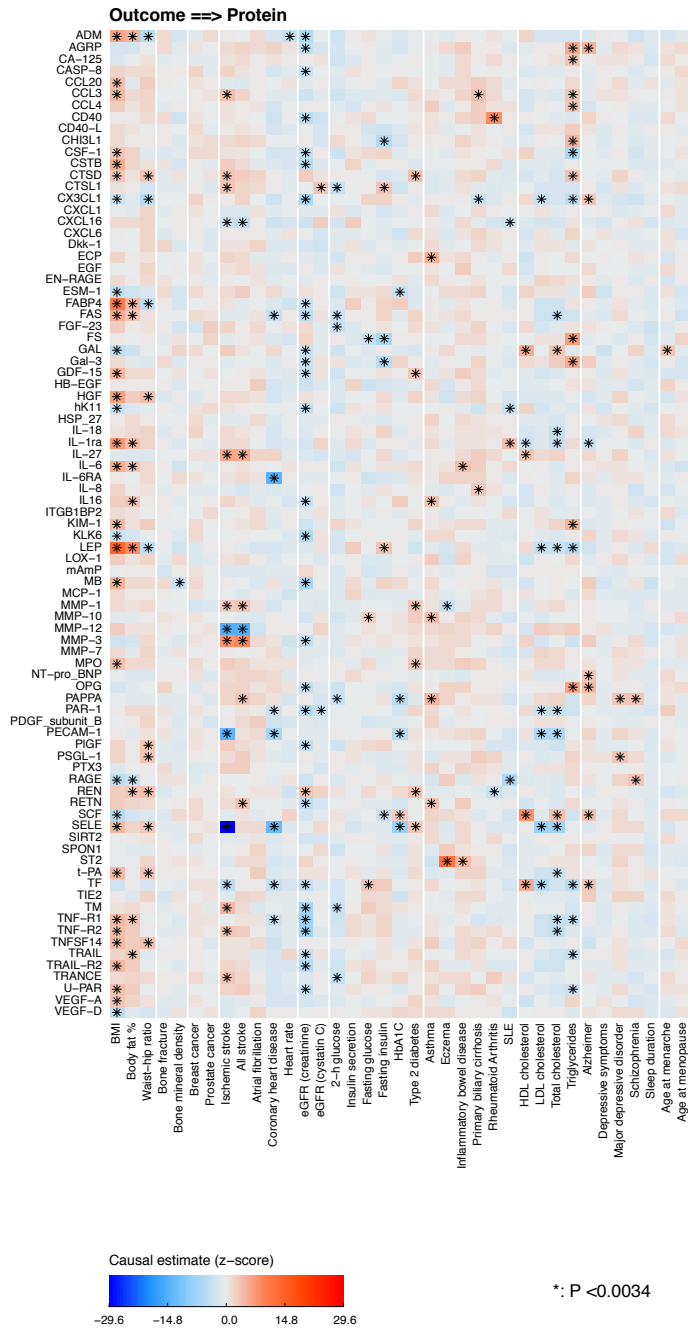


B. MR with strong evidence

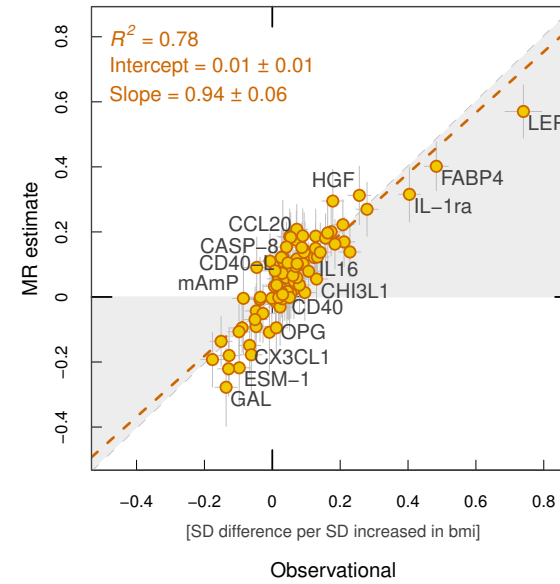


A) ST2 PRS for ST2 in MDC**B) ST2 PRS for asthma in UK-Biobank****C) ST2 PRS for IBD in UK-Biobank**

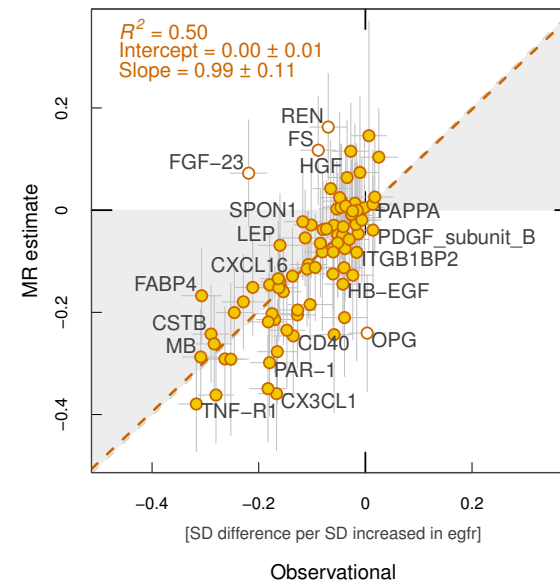
A. 37 traits to 85 proteins



B. BMI ==> proteins: MR vs Observational



C. eGFR ==> proteins: MR vs Observational



Target validation

CASP-8: breast cancer

CD40: IBD, RA

DKK1: eBMD

IL-1RA: RA

IL-6RA: RA, CHD

ST2: asthma

TRAIL-R2: prostate cancer

TRANCE: eBMD

New target candidates

EGF: SCZ, eBMD

IL16: 2h glucose

PAPPA: T2D

SPON1: Afib

TF: HbA1c

Repositioning & target-mediated safety

*(latter denoted by *)*

ADM: WHR

CASP-8: asthma*

CD40: stroke*

CHI3L1: AFib

CSF: WHR, eBMD

CX3CL1: fracture, SLE

CXCL16: IBD

FAS: IBD

GDF-15: HDL-C

HGF: TG

IL-1RA: total cholesterol*

IL-6RA: asthma, eczema*

IL-6RA: AFib

IL18: eBMD

MMP-12: eczema

PIGF: CHD, eBMD

RAGE: Lipids, BMI, T2D,
prostate cancer, SCZ

ST2: IBD*